Electrophilic *As*-Functionalisation of σ–Arsolido complexes

Ryan M. Kirk and Anthony F. Hill*

1 Experimental considerations

1.1 General Precautions

Unless otherwise stated, reactions were carried out under an atmosphere of commercially purified argon or nitrogen using standard Schlenk techniques. Caution should be exercised when handling the tin and arsenic-containing materials described herein – in all cases their toxicological properties are unknown and they are therefore regarded as **toxic**. Metal carbonyls are volatile sources of both carbon monoxide and nanoparticulate metal. Benzene (including benzene-d_6) is a known **carcinogen**. The utmost caution should be exercised when distilling and storing flammable solvents over alkali metals. UV-radiation is non-ionising though ocular protection and suitable shielding should still be in place when sources are active; photolysis of metal carbonyls typically liberates one or more equivalents of carbon monoxide which should be vented appropriately.

1.2 Materials

The arsloyl complexes $[MoAsC_4R_4)(CO)_3(\eta^5\text{-}C_5H_5)]$ R = M, Ph, R_4 = HMe_2SiMe_3) have been described previously.[1] Reagents and materials were obtained from commercial vendors and used as received: alkynes, MeOTf, MeI, neutral alumina, silica gel (230—400 mesh), C_6D_6, CD_2Cl_2 (Cambridge Isotopes Laboratories). HPLC-grade solvents were purchased from Merck and re-purified by distillation under nitrogen from an appropriate desiccant: THF, Et_2O (Na/benzophenone); CH_2Cl_2, $CHCl_3$ (P_2O_5); *n*-pentane, *n*-hexane, *n*-heptane, C_6D_6 (K mirror); CD_2Cl_2 (CaD_2). Solvents for chromatography were degassed with nitrogen and used as received from the same vendor without re-purification.

1.3 Instrumentation.

NMR spectra were collected on Bruker Avance 400, 600, 700 or 800 MHz spectrometers (^{13}C frequencies of 100.6, 150.9, 176.0 and 201.2 MHz respectively). Spectra are reported in ppm shift downfield from $SiMe_4$ and referenced to the residual protio-solvent impurity (^1H: C_6D_6 7.16, CD_2Cl_2 5.32 ppm) or the solvent signal itself (^{13}C: C_6D_6 128.0, CD_2Cl_2 53.8 ppm). ^1H NMR spectra are reported to two decimal places, and ^{13}C to one decimal place. NMR spectra were processed within the MestReNova software package. We thank Dr Doug Lawes of the ANU for assistance and helpful conversation during acquisition of NMR data.

Solution IR were recorded on a Perkin-Elmer Spectrum One FT-IT spectrometer with polished KBr-window cells and wavenumbers are reported to the nearest whole number. Elemental microanalysis was carried out by the Chemical Analysis Facility at Macquarie University (NSW, Australia) and compositions are reported to two decimal places. Data provided are generally the average of dual analyses.

High-resolution ESI mass spectrometry was carried out in positive-ion mode with acetonitrile matrices by the JMSF service at the Research School of Chemistry, ANU, using a Waters Synapt G2-Si HDMS LC-Q/TOF MS-MS spectrometer. Ion masses are reported to four decimal places and most-abundant isotopic compositions for non-C,H,O elements are listed in the text. We thank Mrs Anitha Jeyasingham for acquisition of this data and helpful conversation.

1.4 Crystallography.

Single crystal X-ray diffraction was performed on either an Agilent Technologies XCaliber or Supernova/EosS2-CCD diffractometer with graphite monochromated Mo-Kα (λ = 0.71069 Å) or Cu Kα (λ = 1.54184 Å) at 150 K. Selected crystals were mounted in oil on Nylon loops and fixed under a cold stream of nitrogen. Data were processed using the CrysAlisPRO-CCD and -RED software packages.[2] Absorption corrections are stated for each sample separately. The structures were solved within the Olex2[3] software package with SHELXT[4] using intrinsic phasing and refined with SHELXL[4] using full-matrix least-squares against F^2 in an anisotropic (non-hydrogen atoms only) approximation. All hydrogen atom positions were refined by isotropic approximation in a "riding" model with the U_{iso}(H) parameters fixed to 1.2 U_{eq}(C_i) (for methyl hydrogens) or 1.5 U_{eq}(C_i) (for cyclopentadienyl hydrogens), where U_{eq}(C_i) is the equivalent thermal parameter of the carbon atom to which the corresponding H atom is bonded. Crystal structures were analysed and POV-RAY images rendered within the Mercury 4.3.0 software package.[5] CCDC 2145381-2145383, 2149526, 2145364, 2145367, 2145351 and 2145459 contain the supplementary crystallographic data for this paper and are available free of charge from the Cambridge Crystallographic Data Centre.

1.5 Computational Studies.

Calculations were performed by using the *SPARTAN20*® suite of programs.[6] Geometry optimisation (gas phase) was performed at the DFT level of theory using the exchange functionals ωB97X-D of Head-Gordon,[7,8] The Los Alamos effective core potential type basis set (LANL2Dζ) of Hay and Wadt[9] was used for elements with Z > Kr while Pople 6-31G* basis sets[10] were used for all other atoms. Frequency calculations were performed for all compounds to confirm that each optimized structure was a local minimum, and also to identify vibrational modes of interest. Cartesian atomic coordinates are provided below.

2 Synthetic Procedures

2.1 [Mo(MeAsC$_4$Me$_4$)(CO)$_3$(η^5-C$_5$H$_5$)]OTf ([2a]OTf)

To a solution of [Mo(AsC$_4$Me$_4$)(CO)$_3$(η^5-C$_5$H$_5$)] (**1a**: 0.10 g , 0.23 mmol) in Et$_2$O (5 mL) cooled to 0 °C was added two-to-three drops neat MeOTf (excess. **Caution**: carcinogen) with swirling. Allowing the mixture to stand at ambient temperature without agitation for a few minutes resulted a colour change from orange to yellow with the precipitation of bright yellow crystals. Cooling to -20 °C overnight affected complete crystallisation and the product was collected by decanting the pale-yellow supernatant (**caution**: residual MeOTf) and washing with Et$_2$O (3 x 3 mL portions) and *n*-pentane (2 x 3 mL portions) followed by drying under vacuum. Isolated yield 0.12 g (0.20 mmol, 86%). The salt is readily soluble in polar organic solvents and may be handled in air as a solid or solution for brief periods. Too great an excess of MeOTf should be avoided as it causes decomposition to oily brown residues.

NMR: ^{1}H (CD$_2$Cl$_2$, 400 MHz, 25 °C): δ_H = 5.54 (s, 5 H, C$_5$*H*$_5$), 1.95 (s, 6 H, α-CH$_3$), 1.82 (s, 6 H, β-CH$_3$), 1.66 (s, 3 H, AsCH$_3$) ppm. ^{13}C{^{1}H} (CD$_2$Cl$_2$, 176 MHz, 25 °C): δ_C = 225.8 (*transoid C*O), 223.2 (*cisoid C*O), 145.8 [C^{2,5}(AsC$_4$)]), 134.5 [C^{3,4}(AsC$_4$)], 121.6 (q, $^1J_{FC}$ = 321.2 Hz, CF$_3$SO$_3^-$), 94.3 (C$_5$H$_5$), 14.8 (α-CH$_3$), 13.8 (β-CH$_3$), 11.7 (AsCH$_3$) ppm. IR (CH$_2$Cl$_2$, 25 °C): ν_{CO} = 2057(vs), 1998(sh), 1965(vs) cm^{-1}. IR (CH$_2$Cl$_2$, 25 °C): ν_{CO} = 2045(vs), 1983(s), 1951(vs) cm^{-1}. HR-MS (ESI, MeCN, +ve ion) found *m/z* 444.9686 (calc. for C$_{17}$H$_{20}$O$_3$^{75}As^{98}Mo [*M*]$^+$: 444.9685). Analysis found: C, 36.60; H, 3.41; S, 5.48% (calc. for C$_{18}$H$_{20}$O$_6$AsF$_3$MoS: C, 36.50; H, 3.40; S, 5.41%).

Crystals grown from Et$_2$O solution at -20 °C. C$_{18}$H$_{20}$AsF$_3$MoO$_6$S (*M*$_w$ = 592.26 gmol^{-1}): yellow plate 0.183 × 0.145 × 0.046 mm, triclinic, space group *P*-1 (no. 2), *a* = 8.2247(2) Å, *b* = 8.7800(3) Å, *c* = 15.8527(5) Å, *α* = 98.816(2)°, *β* = 95.151(2)°, *γ* = 93.888(2)°, *V* = 1122.80(6) Å^3, *Z* = 2, analytical correction T_{min}/T_{max} = 0.55803/0.59151, *μ*(Cu-Kα) = 7.804 mm^{-1}, ρ_{calc} = 1.752 Mgm^{-3}, 8310 reflections measured (10.23° ≤ 2Θ ≤ 147.27°), 4447 unique (R_{int} = 0.0298, R_{sigma} = 0.0440) which were used in all calculations, *GOF* = 1.044, D_{min}/D_{max} = -0.59/1.21 eÅ^{-3}. The final R_1 was 0.0331 (I > 2σ(I)) and wR_2 was 0.0866 (all data). CCDC 2145351.

2.2 [Mo{MeAsC$_4$H(SiMe$_3$)Me$_2$}(CO)$_3$(η^5-C$_5$H$_5$)]OTf ([2c]OTf)

Prepared in an identical fashion to that above. Quantities: [Mo{AsC$_4$(H)(SiMe$_3$)Me$_2$}(CO)$_3$(η^5-C$_5$H$_5$)] (**1c**: 0.10 g 0.21 mmol), 2-3 drops neat MeOTf. Obtained as large bright yellow crystals which precipitate from the reaction mixture. Isolated yield: 0.11 g (0.17 mmol, 81%).

NMR: ^{1}H (CD$_2$Cl$_2$, 400 MHz, 25 °C): δ_H = 6.97 (s, 1 H, α-C*H*), 5.81 (s, 5 H, C$_5$H$_5$), 2.23 (s, 3 H, β-CH$_3$), 2.16 (s, 3 H, β-CH$_3$), 1.93 (s, 3 H, AsCH$_3$), 0.31 (s, 9 H, SiCH$_3$) ppm. ^{13}C{^{1}H} (CD$_2$Cl$_2$, 176 MHz, 25 °C): δ_C = 227.5 (*transoid C*O), 225.0 (*cisoid C*O), 224.1 (*cisoid C*O), 161.3 [C^{3,4}(AsC$_4$)], 153.1 [C^{3,4}(AsC$_4$)], 142.1 [C^2(AsC$_4$)], 133.5 [C^5(AsC$_4$)], 121.6 (q, $^1J_{FC}$ = 321.2 Hz, CF$_3$SO$_3^-$), 94.4 (C$_5$H$_5$), 19.4 (β-CH$_3$), 18.7 (β-CH$_3$), 13.0 (As-CH$_3$), 0.8 (SiCH$_3$) ppm. IR (CH$_2$Cl$_2$, 25 °C): ν_{CO} = 2056(vs), 1994(sh), 1971(vs) cm^{-1}. IR (ATR, 25 °C): ν_{CO} = 2045(vs), 1983(s), 1951(vs) cm^{-1}HR-MS (ESI, MeCN, +ve ion) found *m/z* 488.9767 (calc. for C$_{18}$H$_{24}$O$_3$^{75}As^{98}Mo^{28}Si [*M*]$^+$: 488.9770). Analysis found: C, 35.90; H, 3.59; S, 5.11% (calc. for C$_{19}$H$_{24}$O$_6$AsF$_3$MoSSi C, 35.86; H, 3.80; S, 5.04%).

Crystals grown from Et$_2$O solution at -20 °C. C$_{19}$H$_{24}$As$_1$F$_3$Mo$_1$O$_6$S$_1$Si$_1$ (*M*$_w$ = 636.39 gmol^{-1}): yellow prism 0.223 × 0.107 × 0.087 mm, monoclinic, space group *P*2$_1$/*n* (no. 14), *a* = 16.9991(3) Å, *b* = 23.3532(3) Å, *c* = 7.29480(10) Å, *β* = 119.920(3)°, *V* = 2509.95(9) Å^3, *Z* = 4, spherical correction T_{min}/T_{max} = 0.51041/0.54879, *μ*(Cu-Kα) = 7.470 mm^{-1}, ρ_{calc} = 1.684 Mgm^{-3}, 9888 reflections measured (9.664° ≤ 2Θ ≤ 147.312°), 4964 unique (R_{int} = 0.0207, R_{sigma} = 0.0294) which were used in all calculations, *GOF* = 1.027, D_{min}/D_{max} = -0.79/1.50 eÅ^{-3}. The final R_1 was 0.0411 (*I* > 2σ(*I*)) and wR_2 was 0.1108 (all data). CCDC 2145459.

2.3 Reaction between [Mo(AsC$_4$Ph$_4$)(CO)$_3$(η^5-C$_5$H$_5$)] (1b) and CH$_3$I

To a solution of [Mo(AsC$_4$Ph$_4$)(CO)$_3$(η^5-C$_5$H$_5$)] (**1b**: 0.20 g 0.30 mmol) in CH$_2$Cl$_2$ (5 mL) was added two-to-three drops neat CH$_3$I (excess, **Caution**: carcinogen). The mixture was stirred overnight during which time the colour evolved from orange to a deep red. The mixture was absorbed onto a small quantity of neutral alumina by evaporation of the solvent and transferred to a chromatography column of neutral alumina (25 x 1 cm) slurried in petroleum ether. Eluting with 9:1 petroleum ether/Et$_2$O provided a red band of [MoI(CO)$_3$(η^5-C$_5$H$_5$)]. Isolated yield 0.092 g (0.25 mmol, 83%). NMR: ^{1}H (C$_6$D$_6$, 400 MHz, 25 °C): δ_H = 4.44 (s, 5 H, C$_5$H$_5$) ppm. IR (CH$_2$Cl$_2$, 25 °C) ν_{CO} 2043(vs), 1966(vs) cm^{-1}. Identity confirmed by comparison with an authentic sample.

Eluting with 2:1 petroleum ether/CH$_2$Cl$_2$ provided a yellow band of MeAsC$_4$Ph$_4$ (**3**) which was freed of volatiles under reduced pressure and re-crystallised from CH$_2$Cl$_2$/*n*-hexane at -20 °C. Isolated yield 0.095 g (0.21 mmol, 70%).

NMR: ^{1}H (CDCl$_3$, 400 MHz, 25 °C): δ_H = 7.17—7.10 (m, 10 H, C$_6$H$_5$), 7.08-7.40 (m, 6 H, C$_6$H$_5$), 6.92-6.89 (m, 4 H, C$_6$H$_5$), 1.48 (s, 3 H, CH$_3$) ppm. ^{13}C{^{1}H} (CDCl$_3$, 176 MHz, 25 °C): δ_C = 153.8 [C^{2,5}(AsC$_4$)], 149.1 [C^{3,4}(AsC$_4$)], 139.0 (C$_6$H$_5$), 138.5 (C$_6$H$_5$), 130.0 (C$_6$H$_5$), 129.2 (C$_6$H$_5$), 128.1 (C$_6$H$_5$), 127.6 (C$_6$H$_5$), 126.4 (C$_6$H$_5$), 10.0 (CH$_3$) ppm. HR-MS (EI, MeCN, +ve ion) found *m/z* 466.1006 (calc. for C$_{29}$H$_{23}$^{75}As [*M*]$^+$: 446.1010). Analysis found: C, 78.07; H, 5.28% (calc. for C$_{29}$H$_{23}$As: C, 78.02; H, 5.19%).

Crystals grown from CH$_2$Cl$_2$/*n*-hexane at -20 °C; the As-CH$_3$ moiety was disordered over two positions by inflection about the mean arsole ring plane (refined occupancy ratio *ca* 89:11) and was modelled accordingly. C$_{29}$H$_{23}$As (*M*$_w$ = 446.39 gmol^{-1}): yellow prism 0.204 × 0.143 × 0.083 mm, tetragonal, space group *I*4$_1$/*a* (no. 88), *a* = 26.5014(2) Å, *c* = 12.16700(10) Å, *V* = 8545.18(15) Å^3, *Z* = 16, empirical correction T_{min}/T_{max} = 0.96719/1.00000, *μ*(Cu-Kα) = 2.230 mm^{-1}, ρ_{calc} = 1.388 Mgm^{-3}, 11604 reflections measured (7.996° ≤ 2Θ ≤ 147.138°), 4256 unique (R_{int} = 0.0137, R_{sigma} = 0.0168) which were used in all calculations, *GOF* = 1.173, D_{min}/D_{max} = -0.30/0.69 eÅ^{-3}. The

final R_1 was 0.0399 ($I > 2\sigma(I)$) and wR_2 was 0.1001 (all data). CCDC 2149526.

2.4 Reaction between [Mo(AsC$_4$Me$_4$)(CO)$_3$(η^5-C$_5$H$_5$)] and CH$_3$I

To a solution of [Mo(AsC$_4$Me$_4$)(CO)$_3$(η^5-C$_5$H$_5$)] (0.15 g , 0.35 mmol) in *ca* 1 mL of C_6D_6 was added one-to-two drops neat CH_3I (excess). Over the course of *ca* 5 minutes the colour began to change from orange to a deep red, and after standing overnight large colourless crystals separated. The supernatant was decanted, and the crystals washed with Et_2O (3 x 2 mL) and *n*-pentane (2 x 2 mL) and dried under vacuum. Yield: 0.076 g (0.22 mmol, 62%). [Me$_2$AsC$_4$Me$_4$]I ([**4**]I) may be handled for a short while in air, however in solution it decomposes to oily brown residues overnight; the solid crystals are unchanged in air overnight however gain a brown cast over several days. The same cation (as the triflate salt) was similarly obtained by treatment of Et_2O solutions of MeAsC$_4$Me$_4$ with neat MeOTf at 0 °C.

NMR: ^{1}H ($CDCl_3$, 400 MHz, 25 °C): δ_H = 2.58 (s, 6 H, $AsCH_3$), 2.32 (s, 6 H, α-CH_3), 2.00 (s, 6 H, β-CH_3) ppm. ^{13}C{^{1}H} ($CDCl_3$, 176 MHz, 25 °C): δ_C = 150.3 [$C^{2,5}$(AsC$_4$)], 123.5 [$C^{3,4}$(AsC$_4$)], 15.0 (α-CH_3), 14.2 (β-CH_3), 9.28 ($AsCH_3$) ppm. HR-MS (ESI, MeCN, +ve ion) found *m*/*z* 213.0628 (calc. for $C_{10}H_{18}{}^{75}As$ [*M*]$^+$: 213.0625). Analysis found: C, 35.39; H, 5.36% (calc. for $C_{10}H_{18}AsI$: C, 35.32; H, 5.34%).

Crystals grown from C_6D_6 solution at ambient temperature. $C_{10}H_{18}AsI$ (M_w = 340.06 gmol^{-1}): colourless prism 0.298 × 0.085 × 0.056 mm, monoclinic, space group $P2_1/c$ (no. 14), a = 7.9883(4) Å, b = 7.6338(3) Å, c = 21.1208(8) Å, β = 91.549(4)°, V = 1287.50(10) Å^3, Z = 4, spherical correction T_{min}/T_{max} = 0.48902/0.50085, μ(Mo-Kα) = 4.995 mm^{-1}, ρ_{calc} = 1.754 Mgm^{-3}, 24274 reflections measured (6.48° ≤ 2Θ ≤ 64.82°), 4258 unique (R_{int} = 0.0406, R_{sigma} = 0.0344) which were used in all calculations, *GOF* = 1.046, D_{min}/D_{max} = -0.56/0.74 eÅ^{-3}. The final R_1 was 0.0322 ($I > 2\sigma(I)$) and wR_2 was 0.0583 (all data). CCDC number 2145381.

The remainder of the red C_6D_6 solution contains [MoI(CO)$_3$(η^5-C$_5$H$_5$)] as the major product (δ 4.44 ppm), [MoMe(CO)$_3$(η^5-C$_5$H$_5$)] (δ 4.41, 0.39 ppm) and tentatively [MoI(MeAsC$_4$Me$_4$)(CO)$_2$(η^5-C$_5$H$_5$)] (**5**) as the minor species (δ_H = 4.74 ppm; the specific isomer (*cis* or *trans*) is not known) in an approximate ratio of 1:0.14:0.06, , respectively, by ^{1}H NMR integration (η^5-C$_5$H$_5$). No convincing evidence for an acyl complex was found (*cf*. *trans*-[Mo{C(O)Me}(PMe$_3$)(CO)$_2$(η^5-C$_5$H$_5$)] ^{1}H (C_6D_6) δ_H = 4.93 (η^5-C$_5$*H*$_5$), 2.90 (C(O)C*H*$_3$) ppm[11]).

Repeating the reaction in *n*-hexane solution at -30 °C provides a mixture of colourless, yellow, and red crystals, all of which were analysed by X-ray diffraction.

[MoI(CO)$_3$(η^5-C$_5$H$_5$)]: crystals grown from *n*-hexane solution at -30 °C. $C_8H_5IMoO_3$ (M_w = 371.96 gmol^{-1}): red prism 0.20 × 0.138 × 0.074 mm, monoclinic, space group $P2_1/n$ (no. 14), a = 10.4658(3) Å, b = 7.8509(2) Å, c = 12.0747(3) Å, β = 90.736(2)°, V = 992.05(5) Å^3, Z = 4, spherical correction T_{min}/T_{max} = 0.57918/0.61017, μ(Cu-Kα) = 35.053 mm^{-1}, ρ_{calc} = 2.490 Mgm^{-3}, 3425 reflections measured (11.118° ≤ 2Θ ≤ 146.448°), 1924 unique (R_{int} = 0.0343, R_{sigma} = 0.0457) which were used in all calculations, *GOF* = 1.054, D_{min}/D_{max} = -2.02/2.29 eÅ^{-3}. The final R_1 was 0.0464 ($I > 2\sigma(I)$) and wR_2 was 0.1216 (all data). CCDC 2145382.

[MoMe(CO)$_3$(η^5-C$_5$H$_5$)]: This complex was identified by agreement with the unit cell dimensions reported by Valente.[12] Monoclinic $P2_1$ (no. 4), a = 7.5663(4) Å, b = 7.7019(4) Å, c = 8.2091(4) Å, β = 96.837(3), V = 474.98(4) Å^3.

***Cis*-[MoI(MeAsC$_4$Me$_4$)(CO)$_3$(η^5-C$_5$H$_5$)]:** (*cis*-**5**) crystals grown from *n*-hexane solution at -30 °C; two independent molecules were found in the asymmetric unit. $C_{16}H_{20}AsIMoO_2$ (M_w = 542.08 gmol^{-1}): red prism 0.285 × 0.217 × 0.142 mm, triclinic, space group *P*-1 (no. 2), a = 8.8572(3) Å, b = 13.9206(4) Å, c = 16.0715(5) Å, α = 104.867(3)°, β = 104.316(3)°, γ = 91.742(2)°, V = 1846.43(11) Å^3, Z = 4, spherical correction T_{min}/T_{max} = 0.46185/0.50578, μ(Cu-Kα) = 20.938 mm^{-1}, ρ_{calc} = 1.950 Mgm^{-3}, 11500 reflections measured (7.562° ≤ 2Θ ≤ 146.734°), 7149 unique (R_{int} = 0.0306, R_{sigma} = 0.0444) which were used in all calculations, *GOF* = 1.067, D_{min}/D_{max} = -1.64/1.13 e/Å^3 . The final R_1 was 0.0355 ($I > 2\sigma(I)$) and wR_2 was 0.0927 (all data). CCDC 2145383.

***trans*-[Mo{C(O)Me}(MeAsC$_4$Me$_4$)(CO)$_2$(η^5-C$_5$H$_5$)] (*trans*-6) and *trans*-[MoI(MeAsC$_4$Me$_4$)(CO)$_2$(η^5-C$_5$H$_5$)] (*trans*-5):** crystals grown from *n*-hexane solution at -30 °C; the complexes are superimposed in a refined occupancy ratio of *ca* 89:11, respectively. $C_{17.7825}H_{22.675}As_1I_{0.1075}MoO_{2.8925}$ (M_w = 467.20 gmol^{-1}): monoclinic, space group $P2_1/c$ (no. 14), a = 8.23480(10) Å, b = 9.7875(2) Å, c = 23.5300(4) Å, β = 97.499(2)°, V = 1880.25(6) Å^3, Z = 4, spherical correction T_{min}/T_{max} = 0.470/0.512, μ(Cu-Kα) = 9.128 mm^{-1}, ρ_{calc} = 1.650 Mgm^{-3}, 6393 reflections measured (7.58° ≤ 2Θ ≤ 145.896°), 3644 unique (R_{int} = 0.0231, R_{sigma} = 0.0345) which were used in all calculations, *GOF* = 1.119, D_{min}/D_{max} = -0.86/0.60 eÅ^{-3}. The final R_1 was 0.0339 ($I > 2\sigma(I)$) and wR_2 was 0.498 (all data).

2.5 [Mo{C(O)CR=CRAsC$_4$Me$_4$}(CO)$_2$(η^5-C$_5$H$_5$)] (R = CO$_2$Me, 7a)

To a stirred solution of [Mo(AsC$_4$Me$_4$)(CO)$_3$(η^5-C$_5$H$_5$)] (**1a**: 0.20 g 0.47 mmol) in CH_2Cl_2 (10 mL) was added *ca* 100 mg neat dimethyl acetylenedicarboxylate (DMAD, 0.75 mmol). The orange colour rapidly darkened over the course of a few minutes. After 15 minutes stirring, the mixture was transferred to a short column of Florisil® (10 x 1 cm) slurried in Et_2O. Eluting with 3:1 Et_2O/CH_2Cl_2, followed by neat CH_2Cl_2 provides an orange-red band which is collected and freed of volatiles under reduced pressure. Isolated yield: 0.23 g (0.40 mmol, 85%). The product is readily soluble in polar organic and aromatic solvents and is reasonably air stable as a solid or in solution. The use of silica gel or alumina for chromatographic supports appeared to decompose the product.

NMR: ^{1}H (C_6D_6, 400 MHz, 25 °C): δ_H = 4.82 (s, 5 H, C_5H_5), 3.45 (s, 3 H, OCH_3), 3.23 (s, 3 H, OCH_3), 1.88 (s, 3 H, α-C*H*$_3$), 1.59 (s, 3 H, α-CH_3), 1.54 (s, 6 H, β-CH_3) ppm. ^{13}C{^{1}H} (C_6D_6, 176

MHz, 25 °C): δ_C = δ 263.3 (acyl CO), 245.6 (terminal CO), 234.7 (terminal CO), 167.1 (CO_2), 165.9 (CO_2), 161.0 (OC-*C*=C), 149.8 (C=*C*-As), 146.5, 146.3 [$C^{2,5}(AsC_4)$], 133.5, 132.9 [$C^{3,4}(AsC_4)$], 91.9 (C_5H_5), 52.1 (OCH_3), 51.9 (OCH_3) 14.5, 14.4 (α-CH_3), 13.4, 13.2 (β-CH_3) ppm. IR (CH_2Cl_2, 25 °C) ν_{CO} 1962(vs), 1889(s), 1732(s), 1605(m), 1580(sh) cm^{-1}. IR (ATR, 25 °C) ν_{CO} = 1950(vs), 1878(vs), 1730(s), 1717(s), 1581(s) cm^{-1} HR-MS (ESI, MeCN, +ve mode) found *m*/*z* 572.9797 (calc. for $C_{22}H_{23}O_7{}^{75}As^{98}Mo$ $[M]^+$: 572.9800). Analysis found: C, 46.31; H, 4.16% (calc. for $C_{22}H_{23}O_7AsMo$: C, 46.33; H, 4.07%).

Crystals grown from evaporation of an Et_2O solution at -20 °C. $C_{22}H_{23}AsMoO_7$ (M_w = 570.26 $gmol^{-1}$): orange prism 0.416 × 0.156 × 0.07 mm, triclinic, space group *P*-1 (no. 2), *a* = 8.3557(3) Å, *b* = 8.5540(2) Å, *c* = 15.9822(6) Å, *α* = 80.769(3)°, *β* = 87.205(3)°, *γ* = 81.552(2)°, *V* = 1114.92(6) $Å^3$, *Z* = 2, empirical correction 0.80946/1.00000, *μ*(Mo-Kα) = 2.101 mm^{-1}, ρ_{calc} = 1.699 Mgm^{-3}, 23753 reflections measured (6.53° ≤ 2Θ ≤ 65.278°), 7225 unique (R_{int} = 0.0354, R_{sigma} = 0.0442) which were used in all calculations, *GOF* = 1.059, D_{min}/D_{max} = -0.63/0.58 $eÅ^{-3}$. The final R_1 was 0.0308 ($I > 2\sigma(I)$) and wR_2 was 0.0678 (all data). CCDC 2145367.

2.6 [Mo{C(O)CR=CRAsC$_4$Me$_4$}(CO)$_2$(η^5-C$_5$H$_5$)] (R = CF$_3$, 7b)

Into a stirred solution of [Mo(AsC_4Me_4)$(CO)_3$(η^5-C_5H_5)] (**1a**: 0.20 g, 0.47 mmol) in CH_2Cl_2 (10 mL) pre-cooled to -78 °C was condensed an excess of hexafluoro-2-butyne (B.P. = -25 °C. **Caution**: **asphyxiant**) by passing a gentle stream of the gas over the cooled surface for *ca* 20 seconds. The flask was stoppered and the mixture was then allowed to slowly warm to ambient temperature (with occasional venting of excess gas). Over the course of *ca* 30 minutes, the orange colour became a more intense orange-red. The mixture was transferred to a short column of Florisil® (10 x 1 cm) and eluted with Et_2O giving a bright orange band which was collected and freed of volatiles under reduced pressure. Isolated yield 0.25 g (0.42 mmol, 90%). The product is readily soluble in polar organic and aromatic solvents and is reasonably air stable as a solid or in solution.

NMR: ^{1}H (C_6D_6, 400 MHz, 25 °C): δ_H = 4.77 (s, 5 H, C_5H_5), 1.89 (s, 3 H, α-CH_3), 1.45 (s, 3 H, α-CH_3), 1.41 (s, 3 H, β-CH_3), 1.39 (s, 3 H, β-CH_3) ppm. $^{13}C\{^1H\}$ (C_6D_6, 176 MHz, 25 °C): δ_C = 261.4 (acyl CO), 243.2 (terminal CO), 233.6 (terminal CO), 159.6 [dd, OC*C*=C, $^2J_{CF}$ = 28.7, $^3J_{CF}$ = 3.5], 147.6, 146.5 [$C^{2,5}(AsC_4)$], 146.4 [qq, C=*C*-As, $^2J_{CF}$ = 37.0, $^3J_{CF}$ = 1.8], 133.2 , 133.0 [$C^{3,4}(AsC_4)$], 124.8 [q, CF_3, $^1J_{CF}$ = 275.8], 121.6 [q, CF_3, $^1J_{CF}$ = 278.7], 93.3 (C_5H_5), 14.4 (α-CH_3), 14.3 (α-CH_3), 13.7 (β-CH_3), 12.9 (β-CH_3) ppm. $^{19}F\{^1H\}$ (C_6D_6, 376 MHz, 25 °C): δ_F = –56.7 (q, $^5J_{FF}$ = 10.2 Hz, 3F), –59.1 (q, $^5J_{FF}$ = 10.2 Hz, 3F) ppm. IR (CH_2Cl_2, 25 °C): ν_{CO} 1968(vs), 1894(s), 1599(m) cm^{-1}. IR (ATR, 25 °C): ν_{CO} 1956(vs), 1885(vs), 1641(w), 1594(s) cm^{-1}. HR-MS (ESI, MeCN, +ve ion) found *m*/*z* 592.9434 (calc. for $C_{20}H_{17}O_3{}^{75}As^{19}F_6{}^{98}Mo$ $[M]^+$: 592.9432). Analysis found: C, 40.54; H, 3.07% (calc. for $C_{20}H_{17}O_3AsF_6Mo$: C, 40.70; H, 2.90%).

Crystals grown from evaporation of Et_2O solution at –20 °C. $C_{20}H_{17}AsF_6MoO_3$ (M_w = 590.20 $gmol^{-1}$): orange plate 0.261 × 0.109 × 0.052 mm, monoclinic, space group $P2_1/n$ (no. 14), *a* = 8.62420(10) Å, *b* = 17.9549(2) Å, *c* = 14.1123(2) Å, *β* = 103.3860(10)°, *V* = 2125.87(5) $Å^3$, *Z* = 4, Gaussian correction T_{min}/T_{max} = 0.333/1.000, *μ*(Cu-Kα) = 7.451 mm^{-1}, ρ_{calc} = 1.844 Mgm^{-3}, 13901 reflections measured (8.106° ≤ 2Θ ≤ 147.496°), 4288 unique (R_{int} = 0.0247, R_{sigma} = 0.0260) which were used in all calculations, *GOF* = 1.049, D_{min}/D_{max} = -1.16/1.06 $eÅ^{-3}$. The final R_1 was 0.0420 ($I > 2\sigma(I)$) and wR_2 was 0.1066 (all data). CCDC 2145364.

3 Notes and references

1 R. M. Kirk and A. F. Hill, *Dalton Trans.*, 2023, **53**, submitted DOI:

2 *CrysAlis PRO*, Agilent Technologies Ltd, Yarnton, Oxfordshire, England, 2014.

3 O. V. Dolomanov, L. J. Bourhis, R. J. Gildea, J. A. K. Howard and H. Puschmann, *J. Appl. Crystallog.*, **2009**, *42*, 339-341.

4 (a) G. M. Sheldrick, *Acta Crystallogr. Sect. A: Found. Crystallogr.*, 2008, **64**, 112; (b) G. M. Sheldrick, *Acta Crystallogr. Sect. C: Cryst. Struct. Commun.*, 2015, 71, 3.

5 (a) C. F. Macrae, P. R. Edgington, P. McCabe, E. Pidcock, G. P. Shields, R. Taylor, M. Towler and J. van de Streek, *J. Appl. Crystallogr.*, 2006, **39**, 453-457. (b) C. F. Macrae, I. J. Bruno, J. A. Chisholm, P. R. Edgington, P. McCabe, E. Pidcock, L. Rodriguez-Monge, R. Taylor, J. van de Streek and P. A. Wood, *J. Appl. Crystallogr.*, 2008, **41**, 466-470.

6 *Spartan 20*® (2020) Wavefunction, Inc., 18401 Von Karman Ave., Suite 370 Irvine, CA 92612 U.S.A.

7 J. D. Chai and M. Head-Gordon, *J Chem Phys.*, 2008, **128**, 084106.

8 J. D. Chai and M. Head-Gordon, *Phys Chem Chem Phys*, 2008, **10**, 6615-6620.

9 (a) P. J. Hay and W. R. Wadt, *J. Chem. Phys.*, 1985, **82**, 270-283. (b) P. J. Hay and W. R. Wadt, *J. Chem. Phys.*, 1985, **82**, 299-310. (c) W. R. Wadt and P. J. Hay, *J. Chem. Phys.*, 1985, **82**, 284-298.

10 W. J. Hehre, R. Ditchfeld and J. A. Pople, *J. Chem. Phys.*, 1972, **56**, 2257–2261.

11 W. Malisch, H. Blau and F. J. Haaf, *Chem. Ber.*, 1981, **114**, 2956-2970.

12 M. Abrantes, P. Neves, M. M. Antunes, S. Gago, F. A. Almeida Paz, A. E. Rodrigues, M. Pillinger, I. S. Gonçalves, C. M. Silva and A. A. Valente, *J. Mol. Cat. A.*, 2010, **320**, 19-26.

4 Selected Spectra

4.1 [Mo(MeAsC$_4$Me$_4$)(CO)$_3$(η^5-C$_5$H$_5$)]OTf [2a]OTf

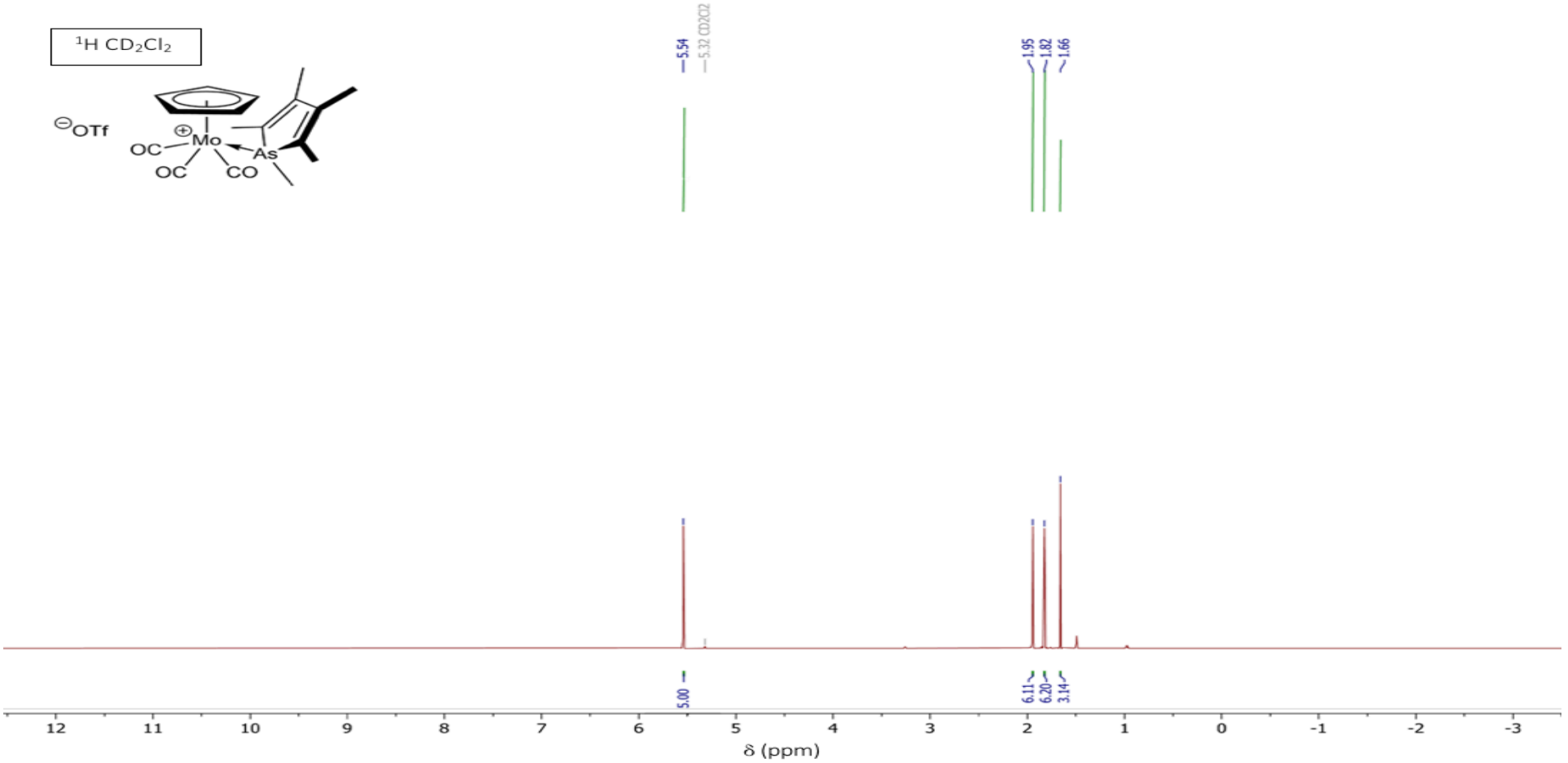

Figure S1. ^{1}H NMR Spectrum (CD_2Cl_2, 295 K, 400 MHz, δ) of [Mo(MeAsC$_4$Me$_4$)(CO)$_3$(η^5-C$_5$H$_5$)]OTf [**2a**]OTf

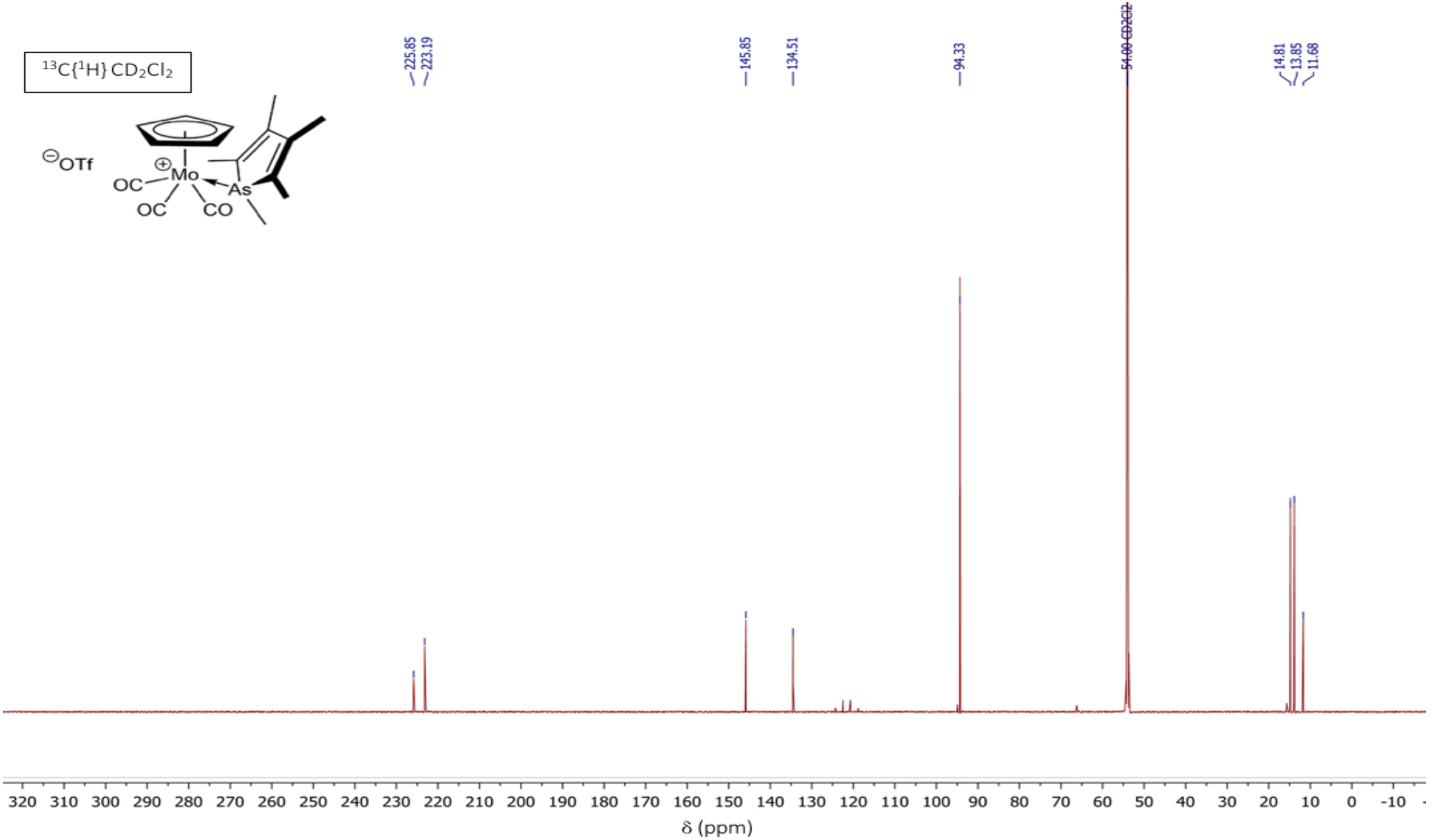

Figure S2. $^{13}C\{^1H\}$ NMR Spectrum (CD_2Cl_2, 295 K, 101 MHz, δ) of [Mo($MeAsC_4Me_4$)$(CO)_3$(η^5-C_5H_5)]OTf [**2a**]OTf

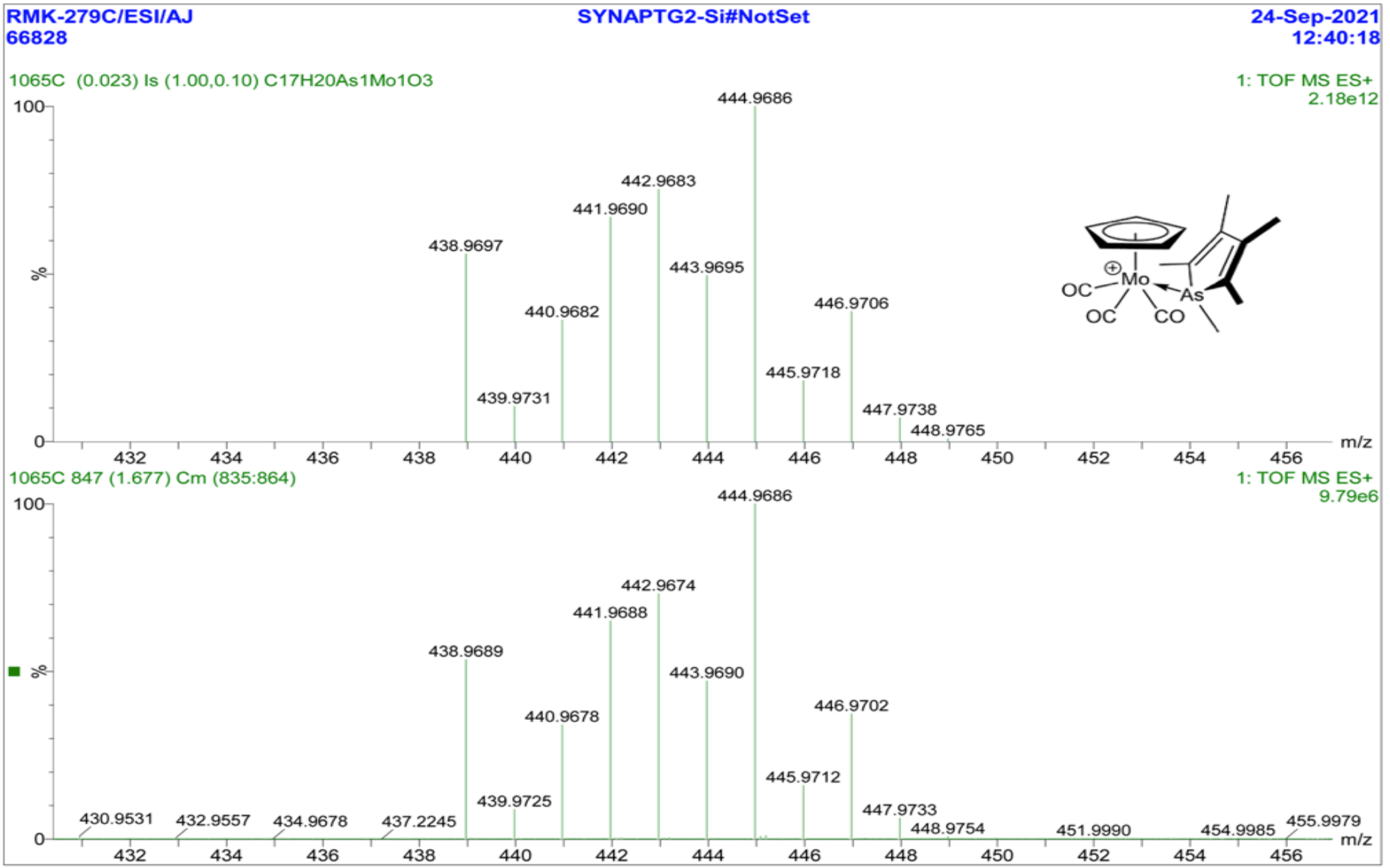

Figure S3. High Resolution Mass Spectrum (ESI-MS, MeCN, +ve ion) of [**2a**]$^+$ obtained from the salt [Mo(MeAsC_4Me_4)$(CO)_3(\eta^5$-$C_5H_5)$]OTf ([**2a**]OTf)

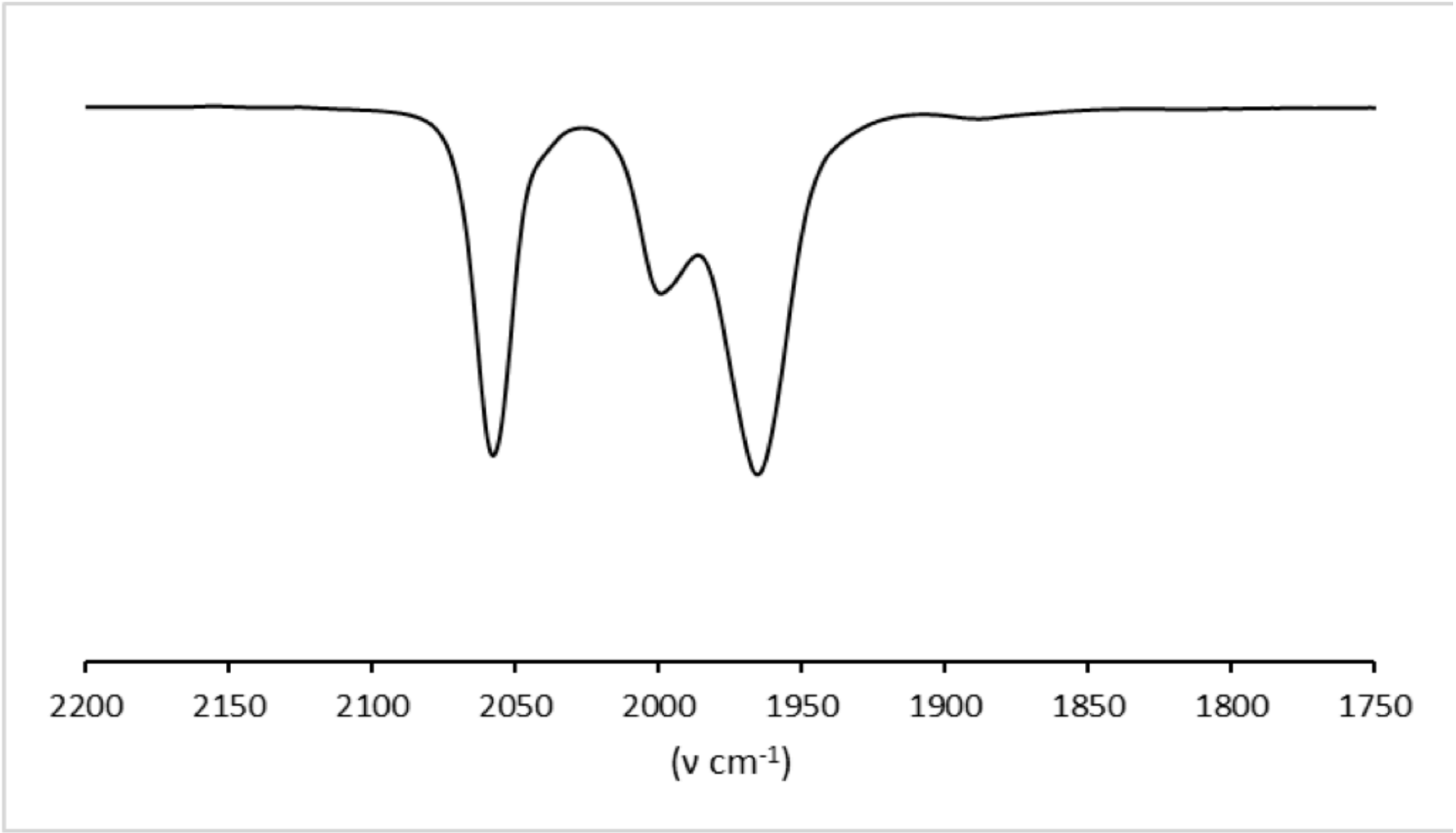

Figure S4. IR Spectrum (CH_2Cl_2, 295 K, ν cm^{-1}) of $Mo(MeAsC_4Me_4)(CO)_3(\eta^5\text{-}C_5H_5)]OTf$ [**2a**]OTf

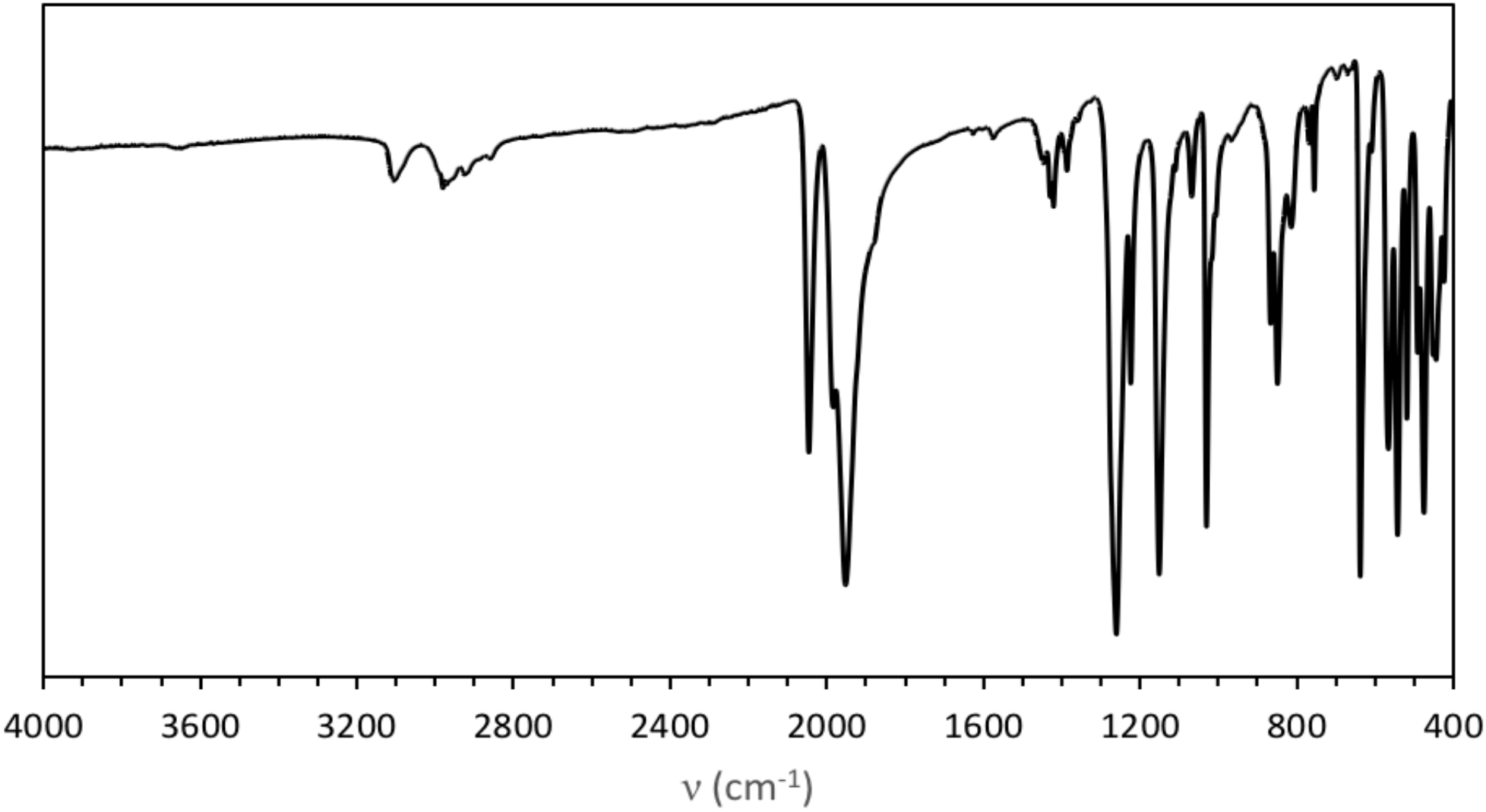

Figure S5. IR Spectrum (ATR, 295 K, ν cm^{-1}) of $Mo(MeAsC_4Me_4)(CO)_3(\eta^5\text{-}C_5H_5)]OTf$ [**2a**]OTf

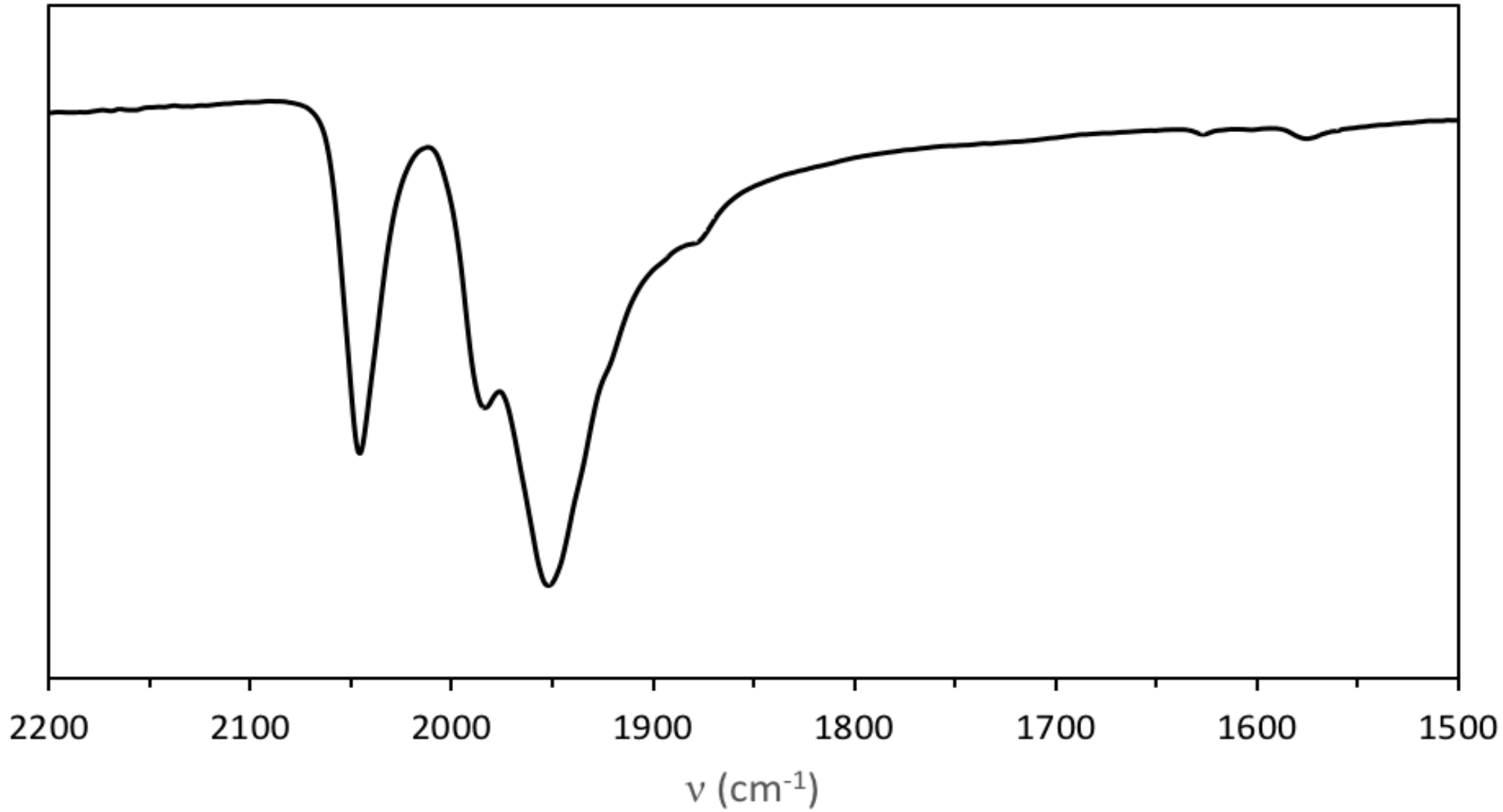

Figure S6. IR Spectrum (ATR, 295 K, ν cm^{-1}) of $Mo(MeAsC_4Me_4)(CO)_3(\eta^5\text{-}C_5H_5)]OTf$ [**2a**]OTf – Expansion of ν_{CO} region.

4.2 [Mo{MeAsC$_4$HMe$_2$-3,4-(SiMe$_3$)-2}(CO)$_3$(η^5-C$_5$H$_5$)]OTf [3a]OTf

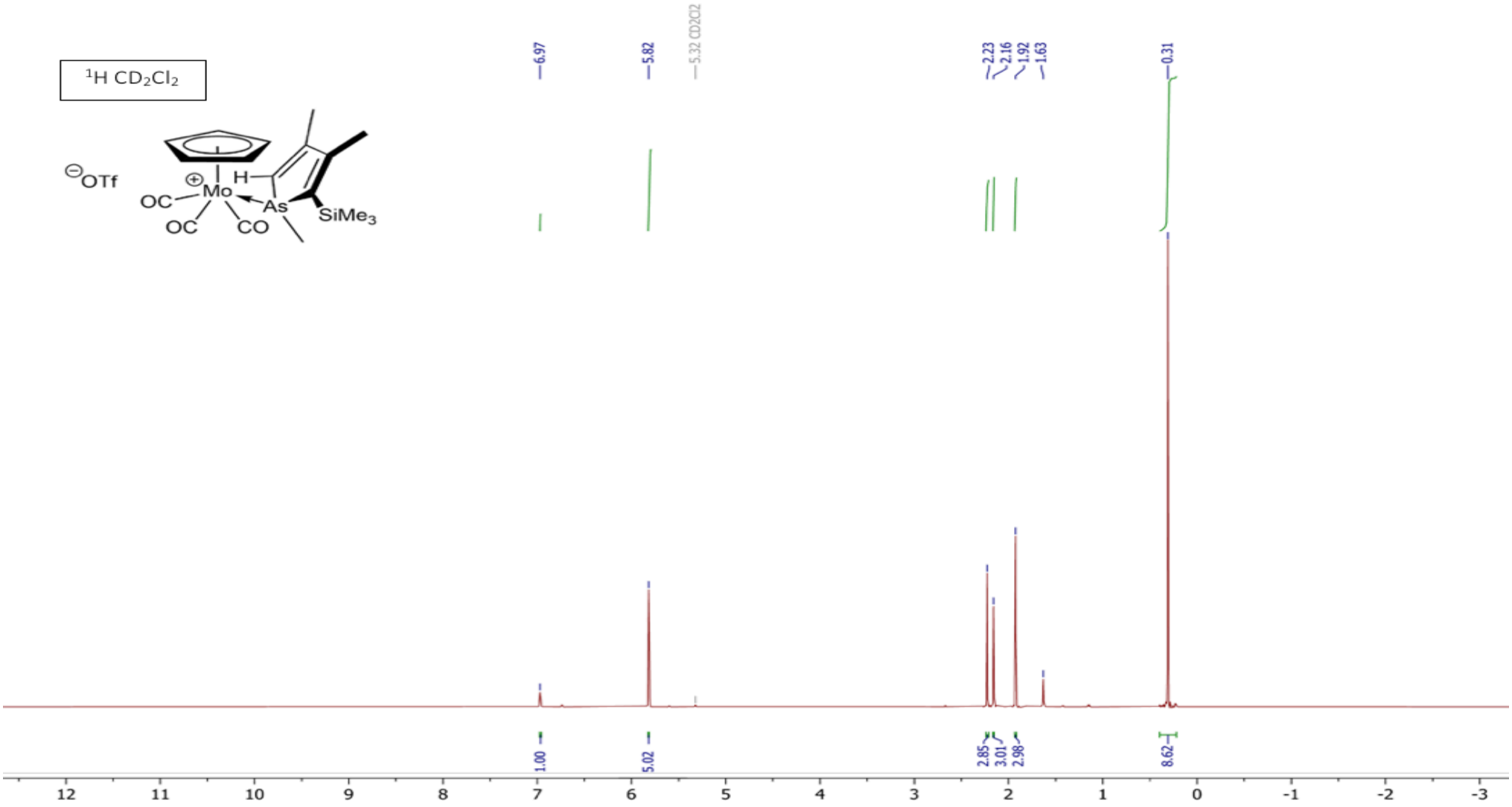

Figure S7. ^{1}H NMR Spectrum (CD_2Cl_2, 295 K, 400 MHz, δ) of Mo{MeAsC$_4$HMe$_2$-3,4-(SiMe$_3$)-2}(CO)$_3$(η^5-C$_5$H$_5$)]OTf [**3a**]OTf

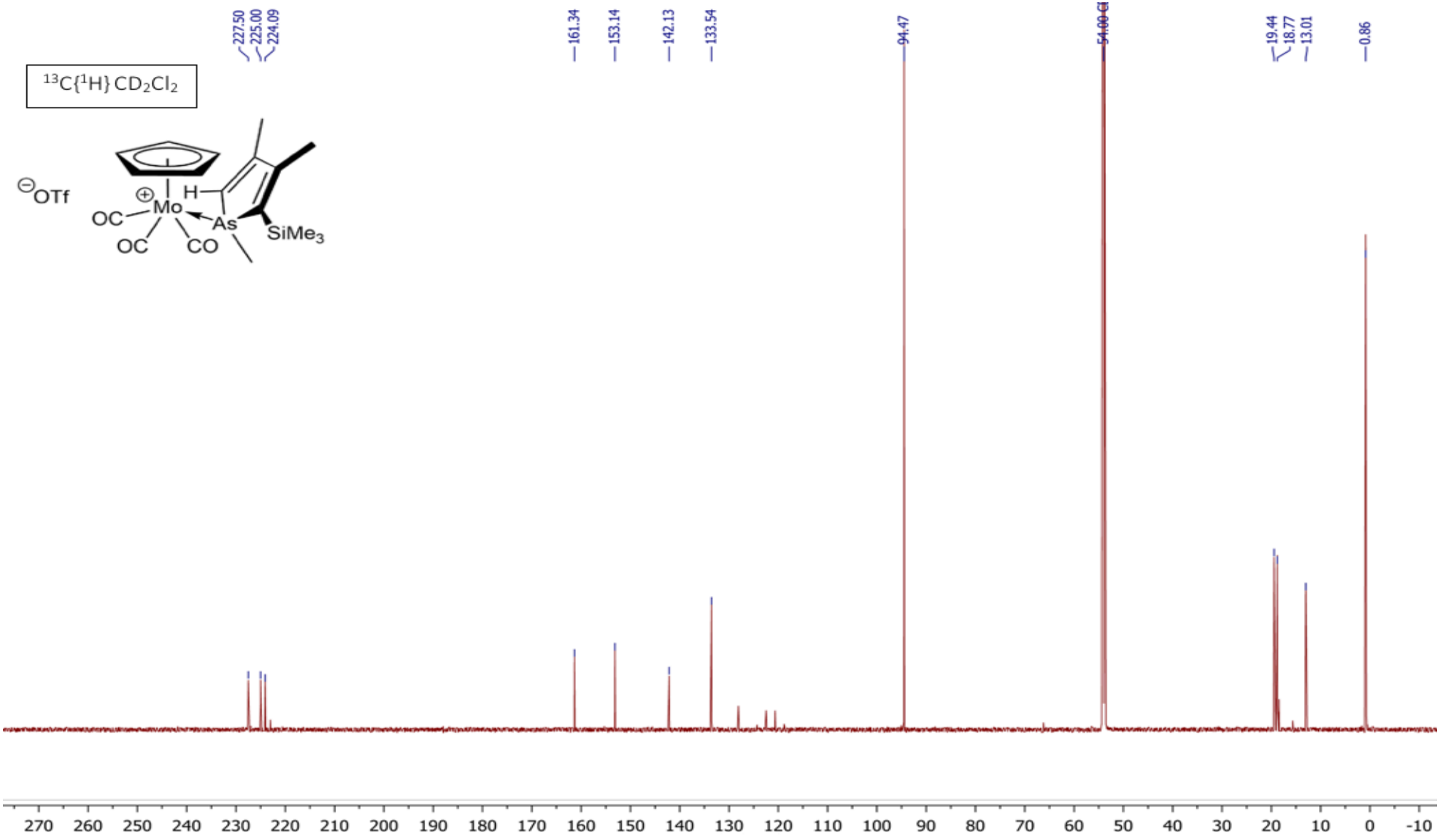

Figure S8. $^{13}C\{^1H\}$ NMR Spectrum (CD_2Cl_2, 295 K, 201 MHz, δ) of Mo{$MeAsC_4HMe_2$-3,4-$(SiMe_3)$-2}$(CO)_3(\eta^5$-$C_5H_5)$]OTf [**3a**]OTf

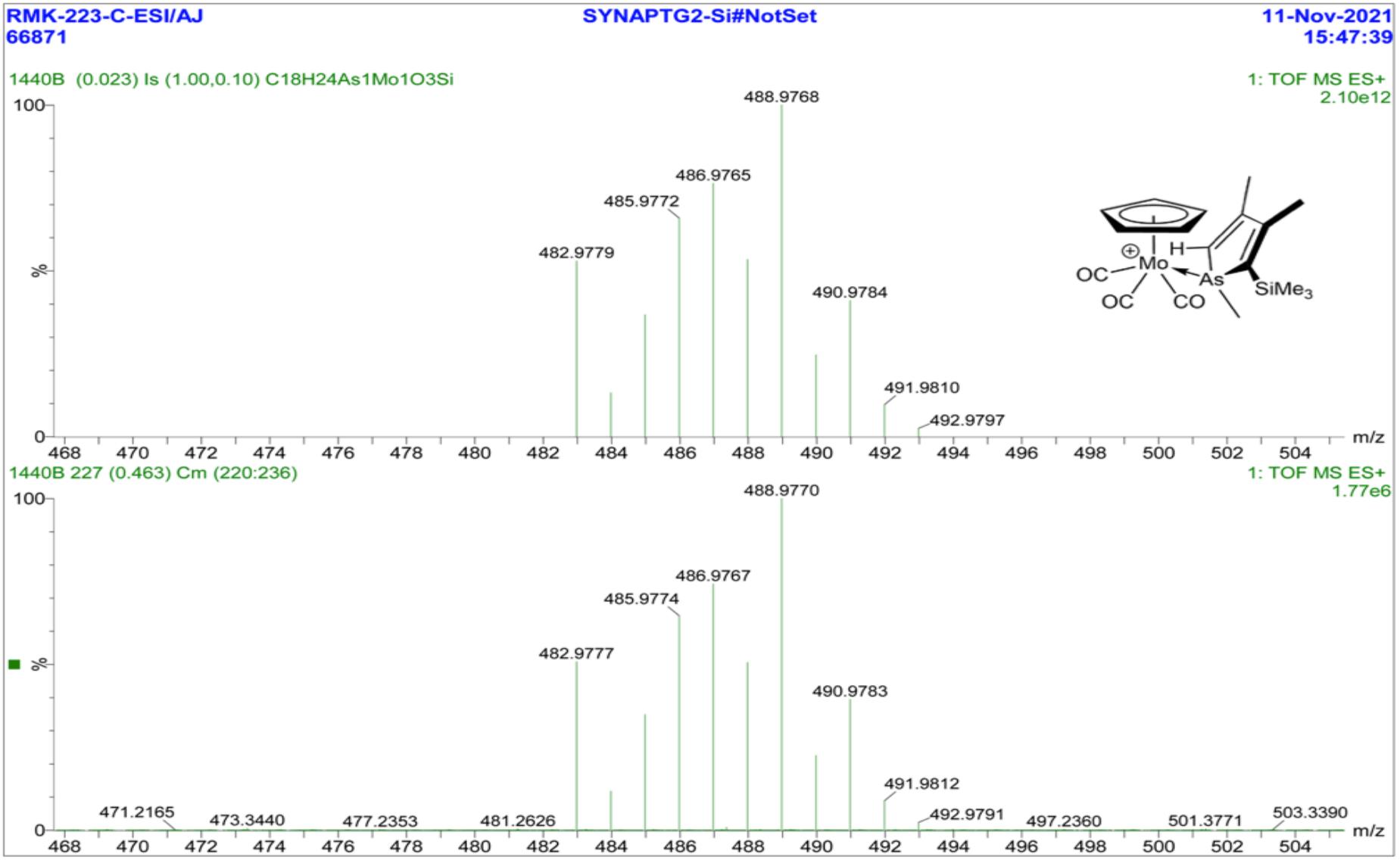

Figure S9. High Resolution Mass Spectrum (ESI-MS, MeCN, +ve ion) of the cation [**2c**]$^+$ obtained from the triflate salt [Mo{MeAsC_4HMe_2-3,4-(SiMe_3)-2}$(CO)_3(\eta^5$-$C_5H_5)$]OTf [**2c**]OTf

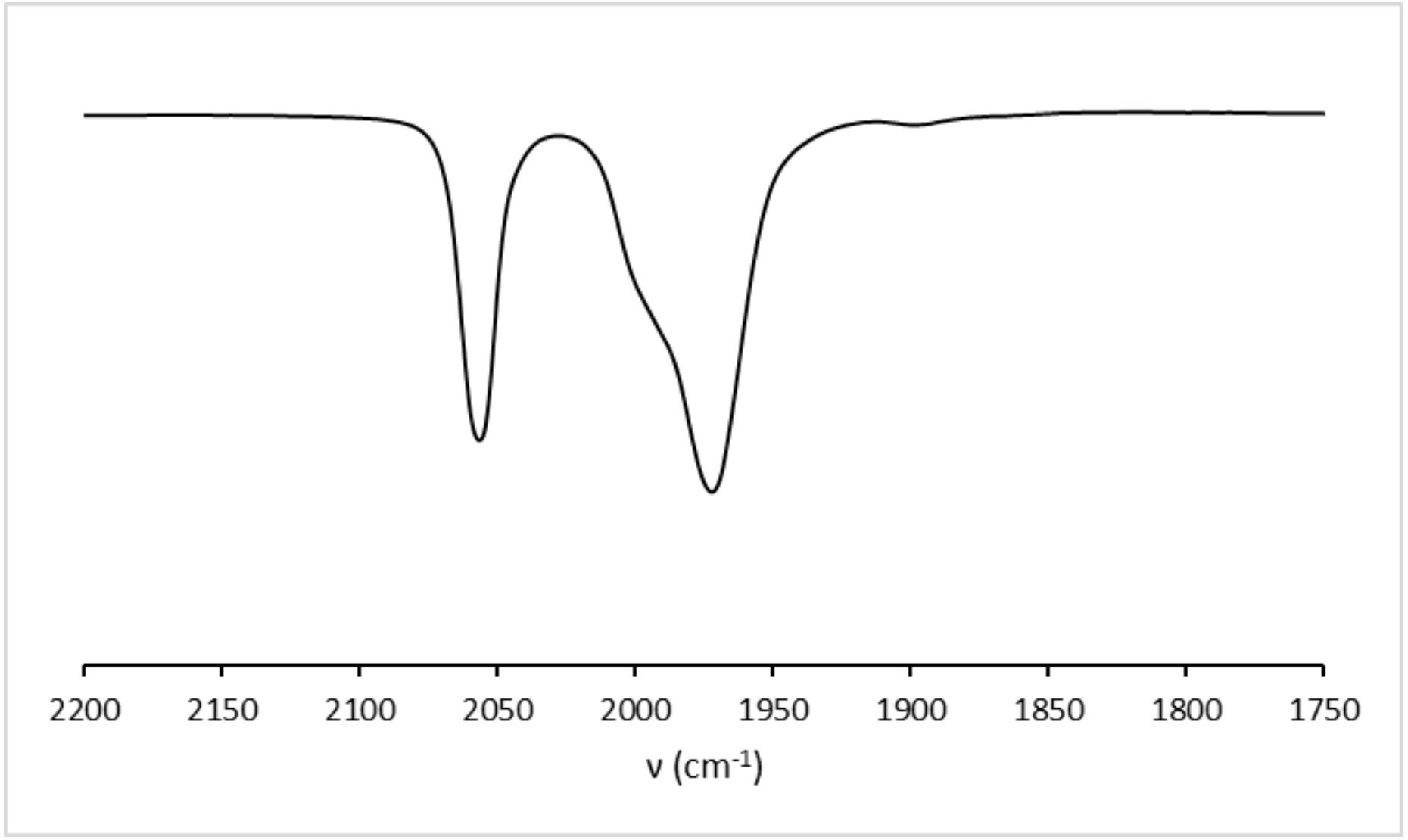

Figure S10. IR Spectrum (CH_2Cl_2, 295 K, ν cm^{-1}) of Mo{$MeAsC_4HMe_2$-3,4-$(SiMe_3)$-2}$(CO)_3(\eta^5$-$C_5H_5)$]OTf [**3a**]OTf

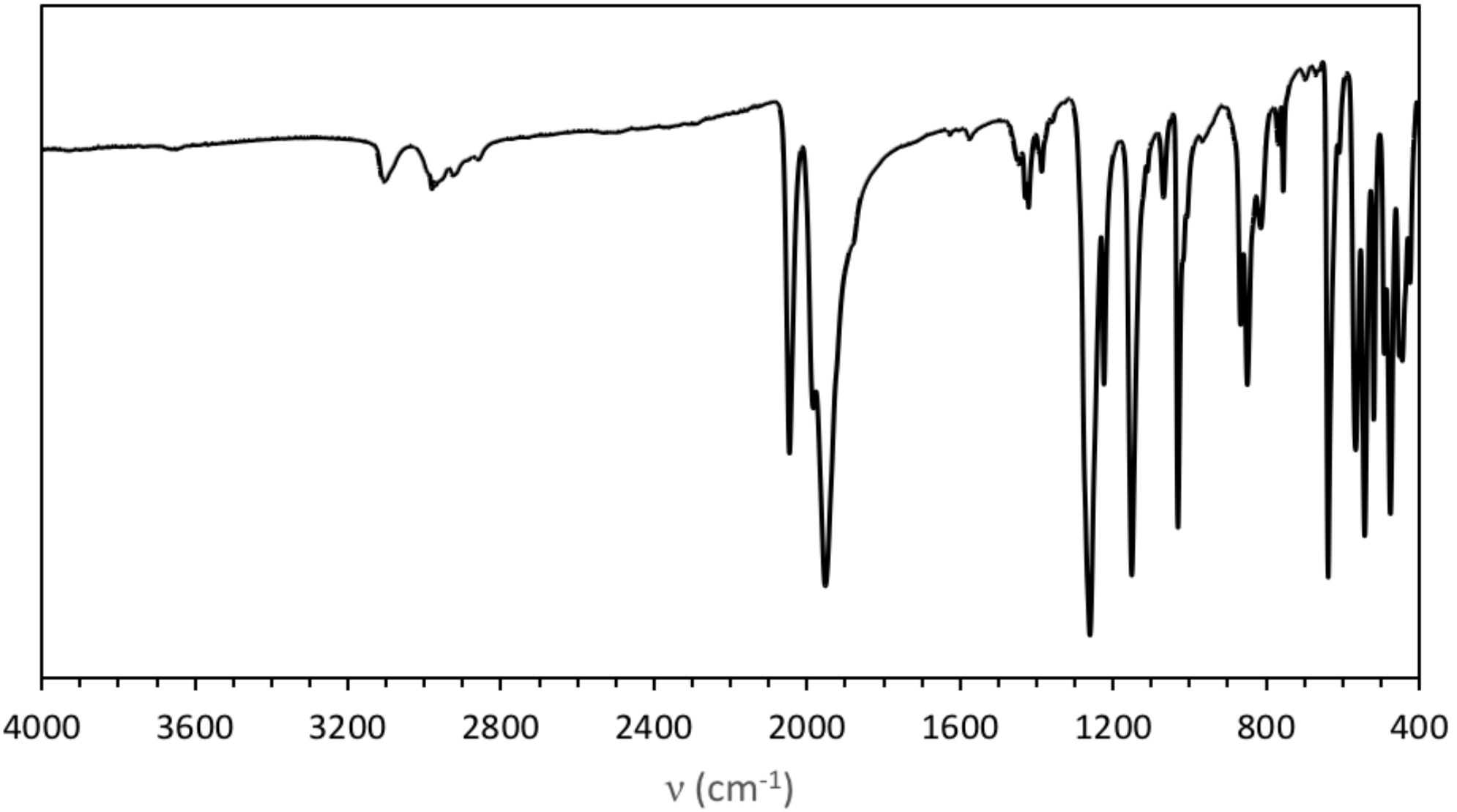

Figure S11. IR Spectrum (ATR, 295 K, ν cm^{-1}) of Mo{$MeAsC_4HMe_2$-3,4-$(SiMe_3)$-2}$(CO)_3(\eta^5$-$C_5H_5)$]OTf [**3a**]OT

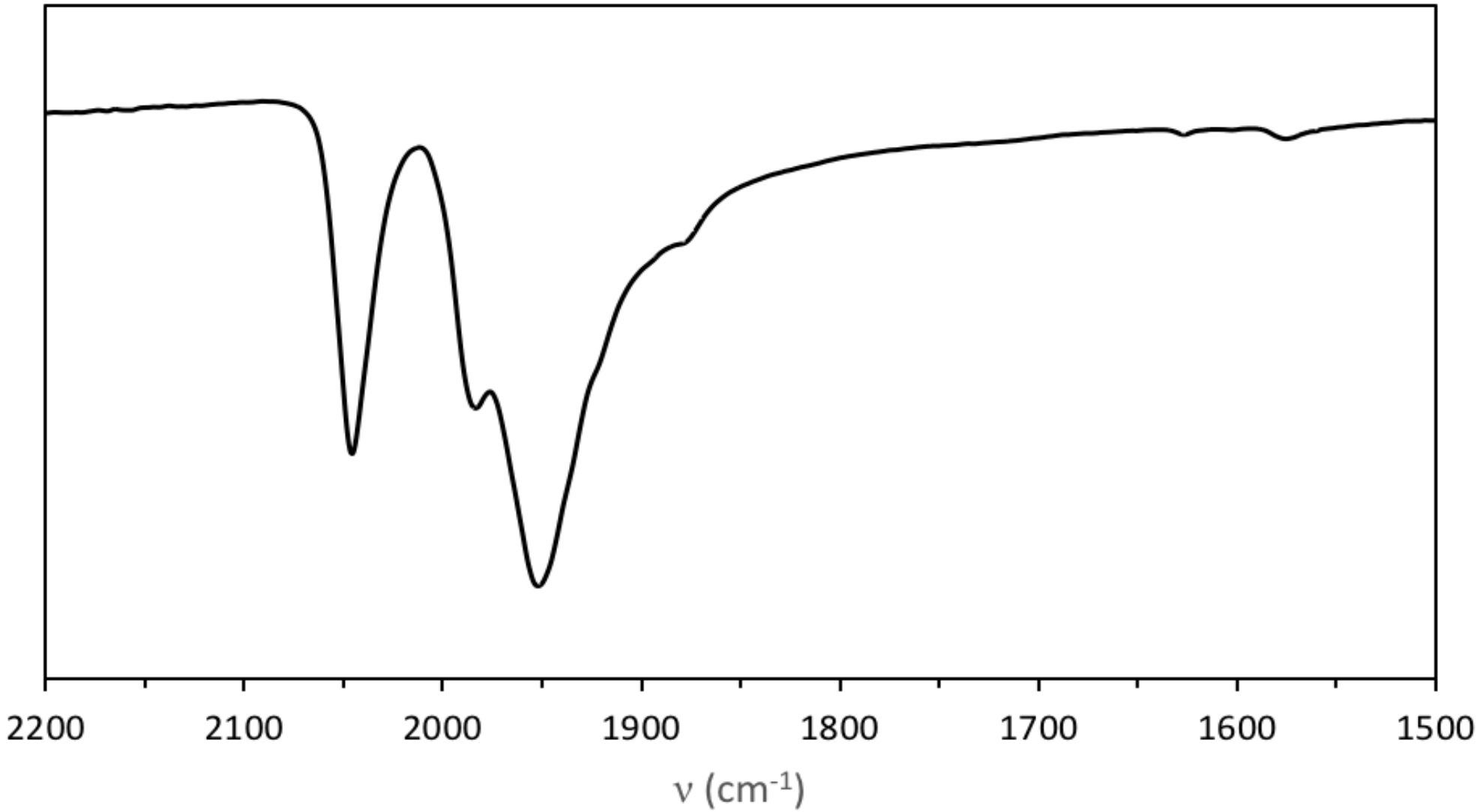

Figure S12. IR Spectrum (ATR, 295 K, ν cm^{-1}) of Mo{$MeAsC_4HMe_2$-3,4-$(SiMe_3)$-2}$(CO)_3(\eta^5$-$C_5H_5)$]OTf [**3a**]OT– Expansion of ν_{CO} region

4.3 $MeAsC_4Ph_4$

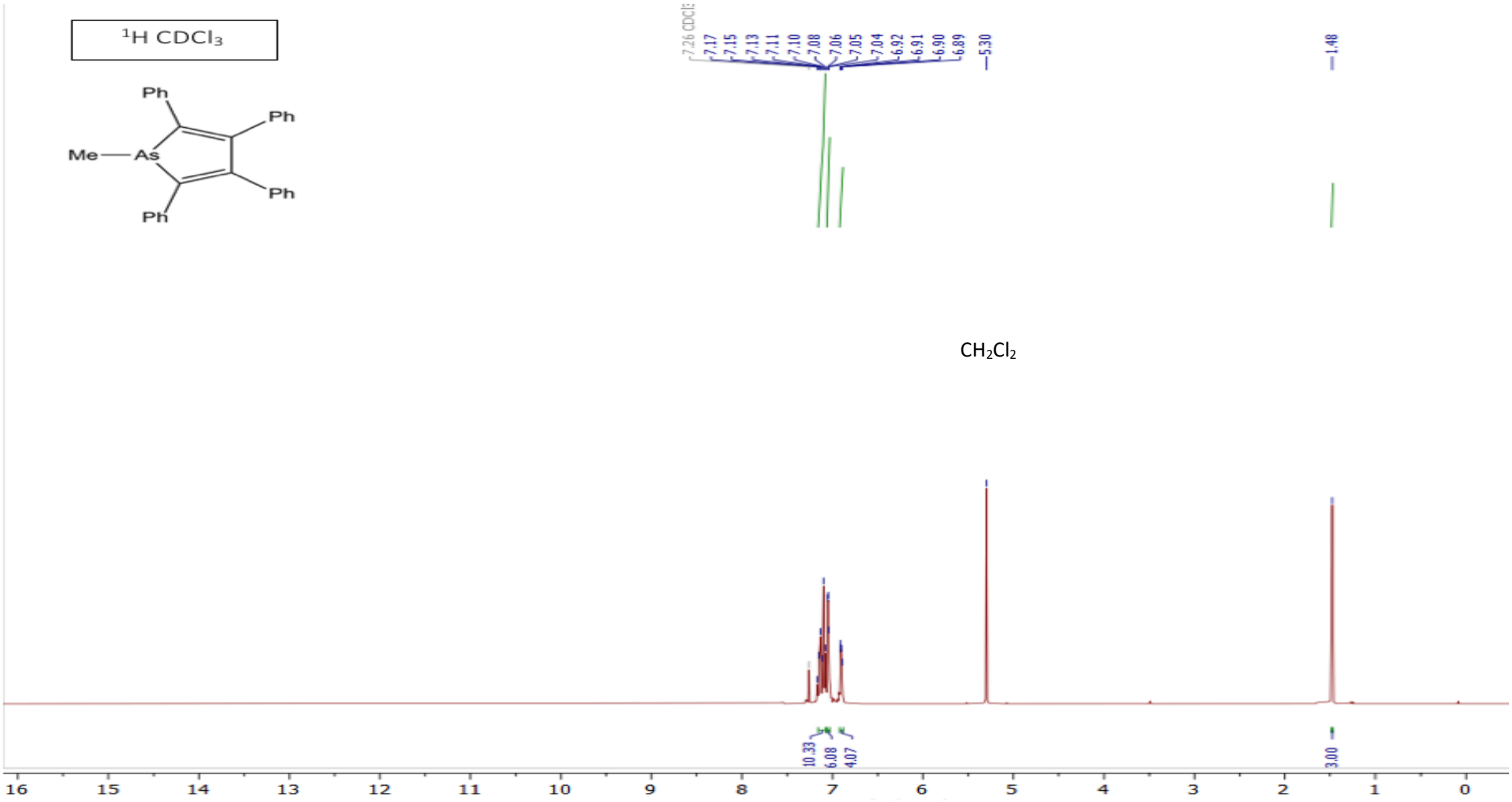

Figure S13. ^{1}H NMR Spectrum ($CDCl_3$, 295 K, 400 MHz, δ) of $MeAsC_4Ph_4$ (**3**)

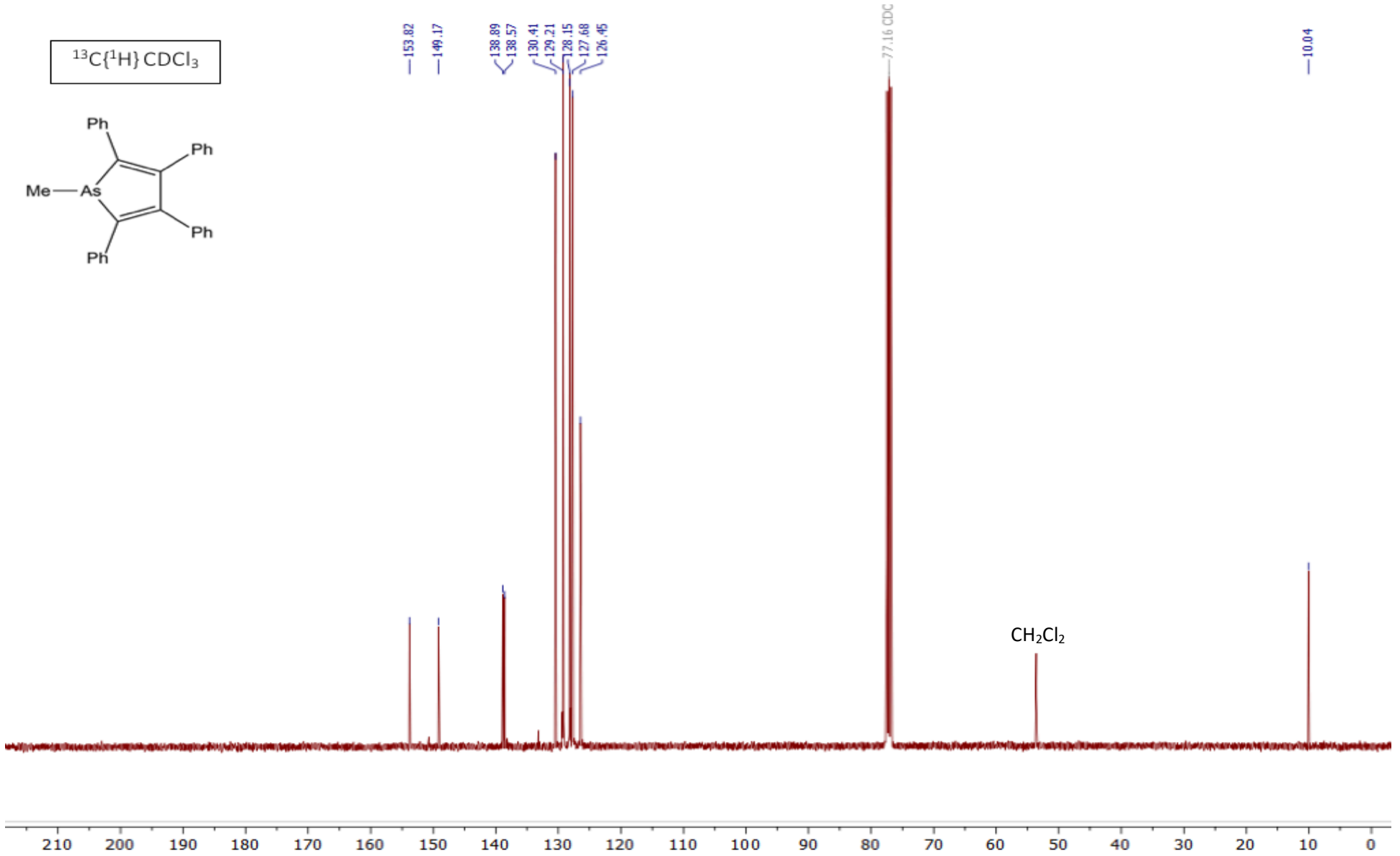

Figure S14. $^{13}C\{^{1}H\}$ NMR Spectrum ($CDCl_3$, 295 K, 201 MHz, δ) of $MeAsC_4Ph_4$ (**3**)

4.4 [$Me_2AsC_4Me_4$]I

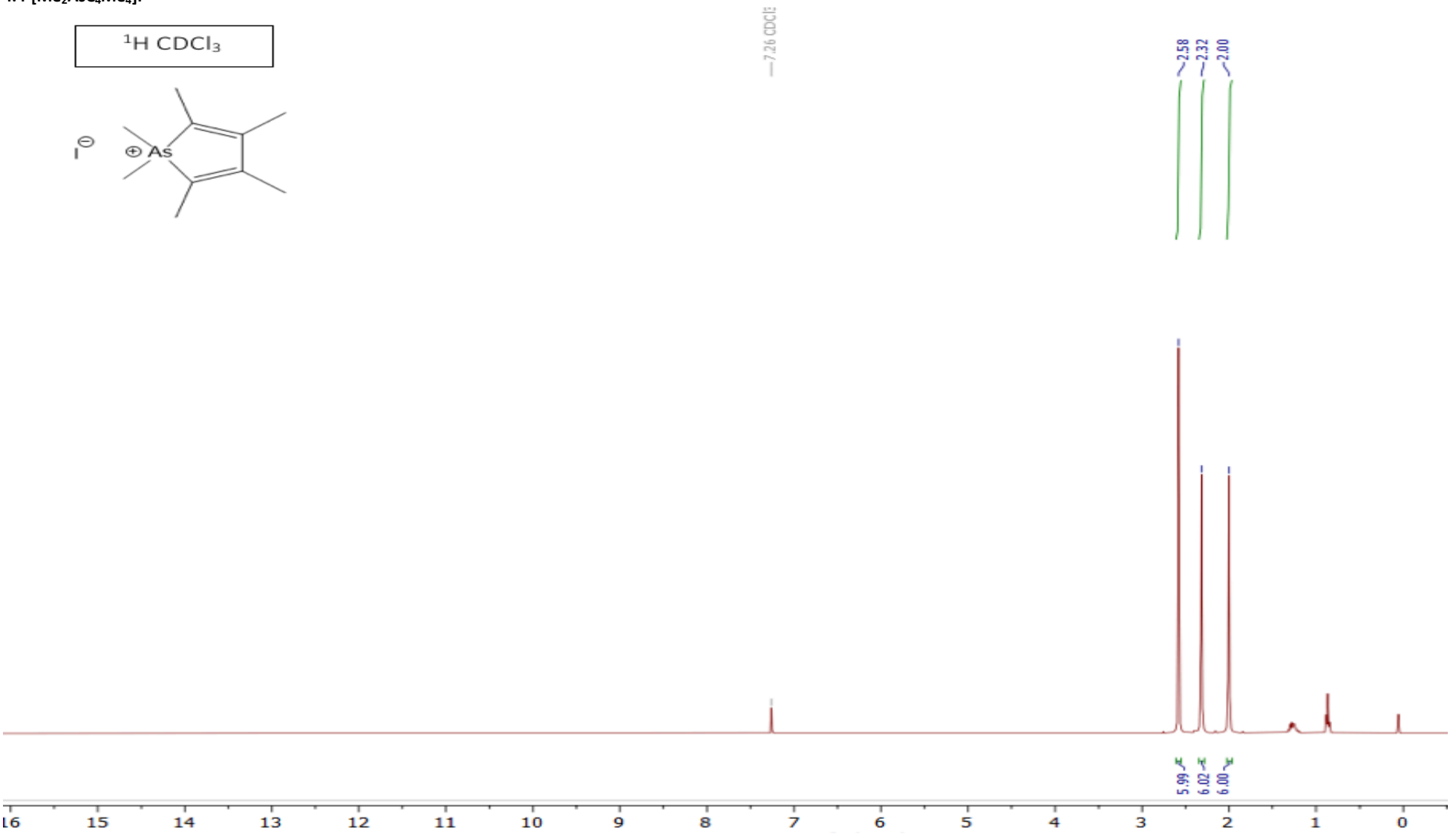

Figure S15. ^{1}H NMR Spectrum ($CDCl_3$, 295 K, 400 MHz, δ) of [$Me_2AsC_4Me_4$]I [**4**]I

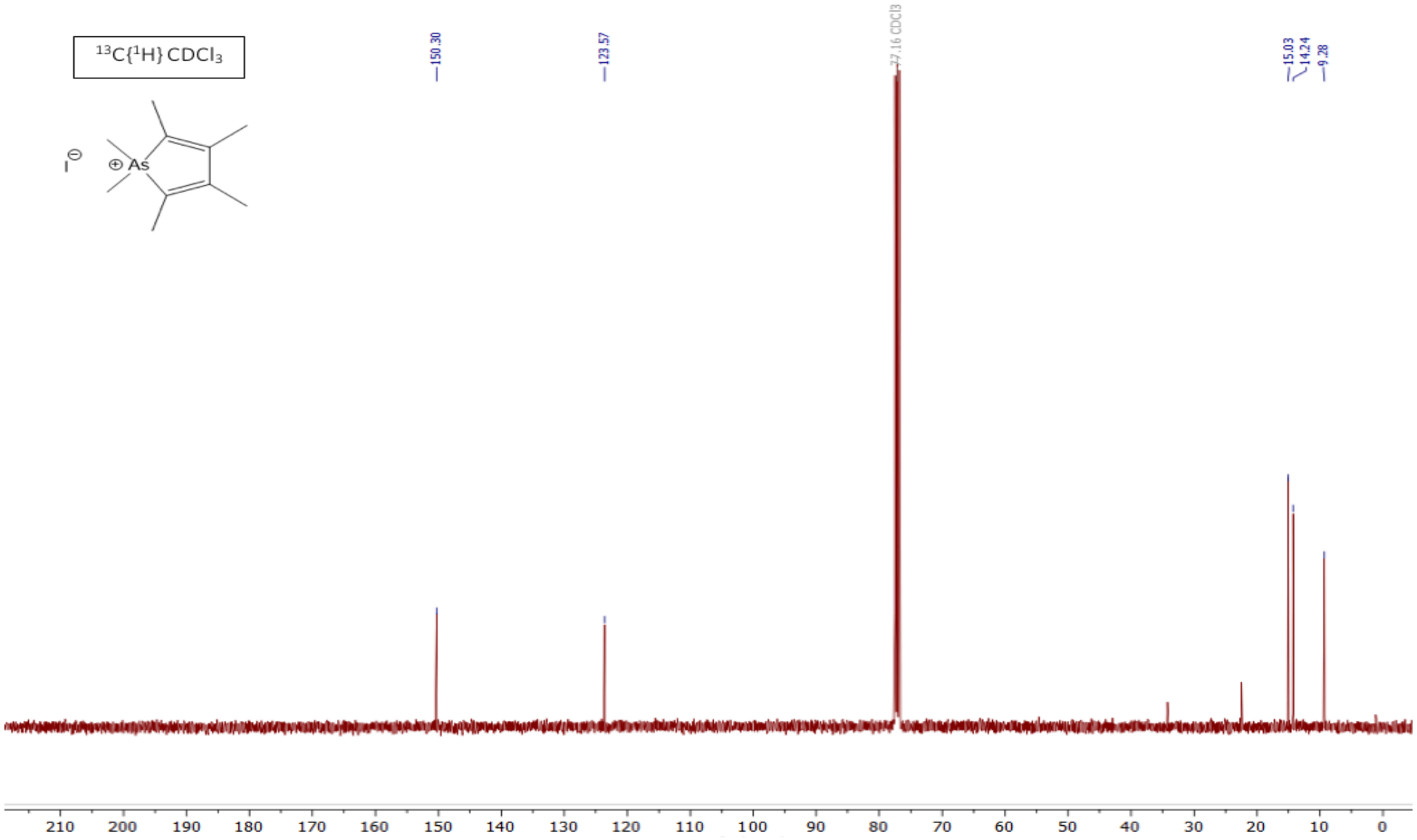

Figure S16. $^{13}C\{^{1}H\}$ NMR Spectrum ($CDCl_3$, 295 K, 101 MHz, δ) of $[Me_2AsC_4Me_4]I$ [**4**]I

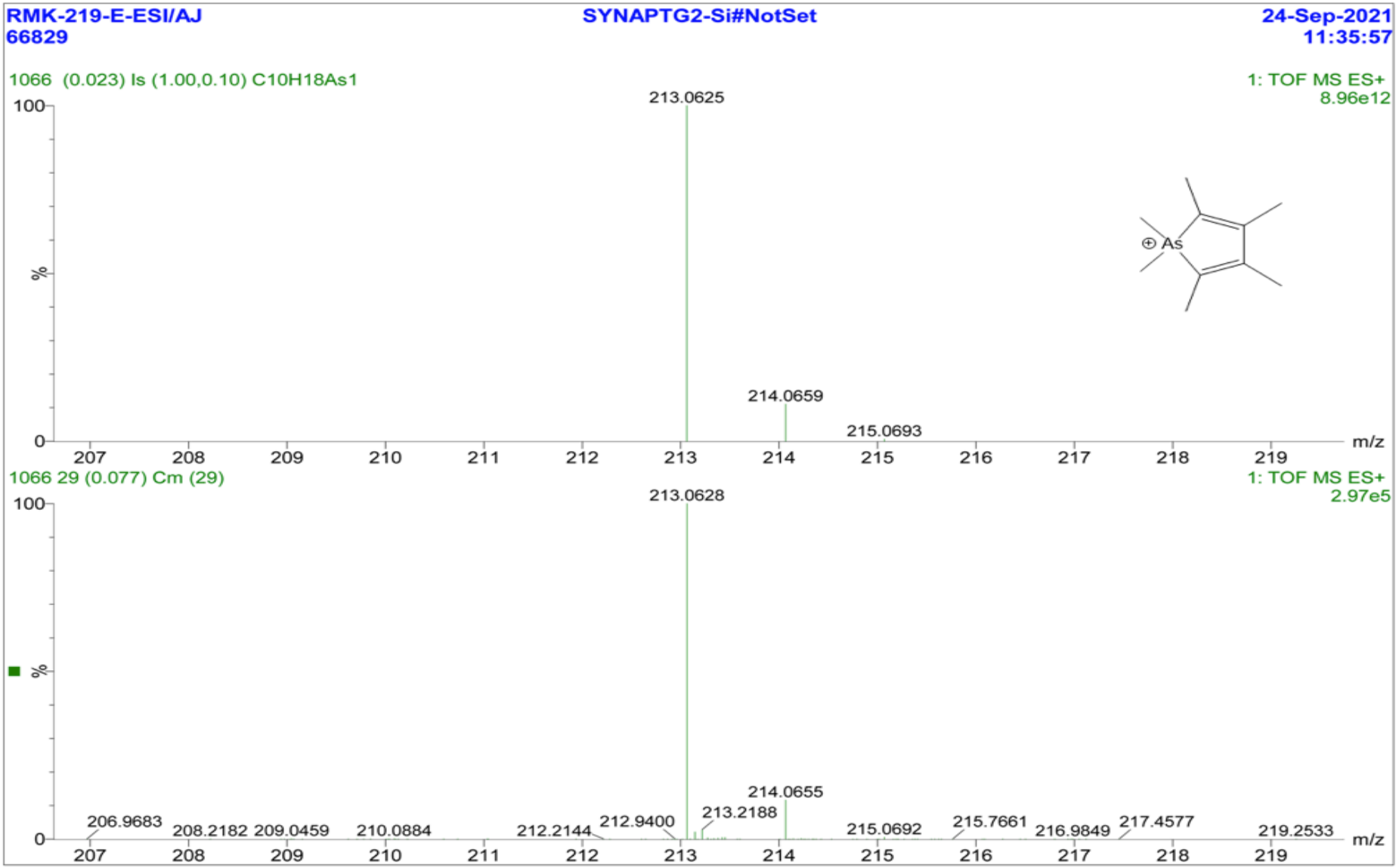

Figure S17. High Resolution Mass Spectrum (ESI-MS, MeCN, +ve ion) of the cation [**4**]$^+$ obtained from the iodide salt [$Me_2AsC_4Me_4$]I [**4**]I

4.5 [Mo{C(O)CR=CRAsC$_4$Me$_4$}(CO)$_2$(η^5-C$_5$H$_5$)] (R = CO$_2$Me, 7a)

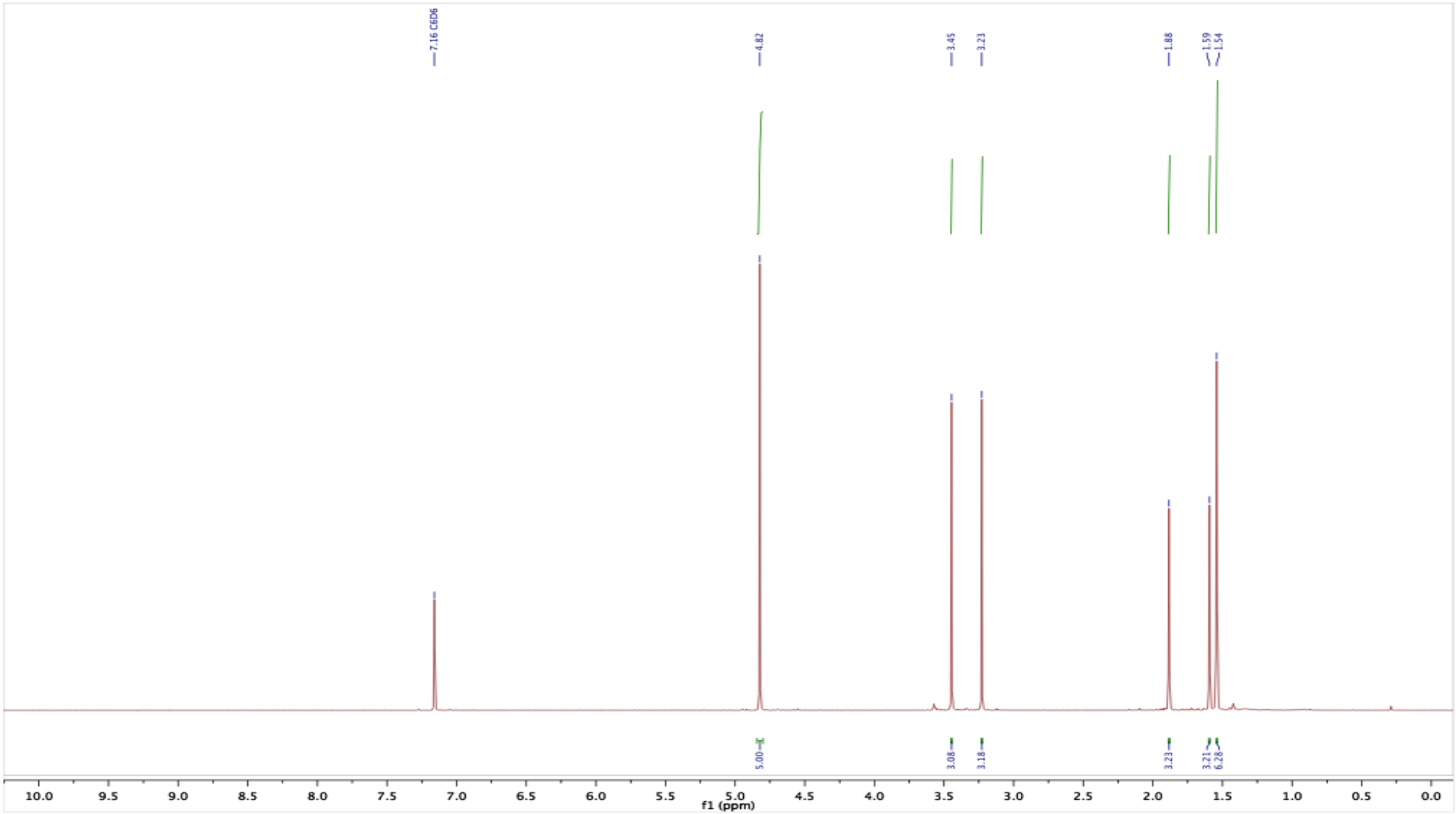

Figure S18. ^{1}H NMR Spectrum (C$_6$D$_6$, 295 K, 400 MHz, δ) of [Mo{C(O)CR=CRAsC$_4$Me$_4$}(CO)$_2$(η^5-C$_5$H$_5$)] (R = CO$_2$Me, **7a**)

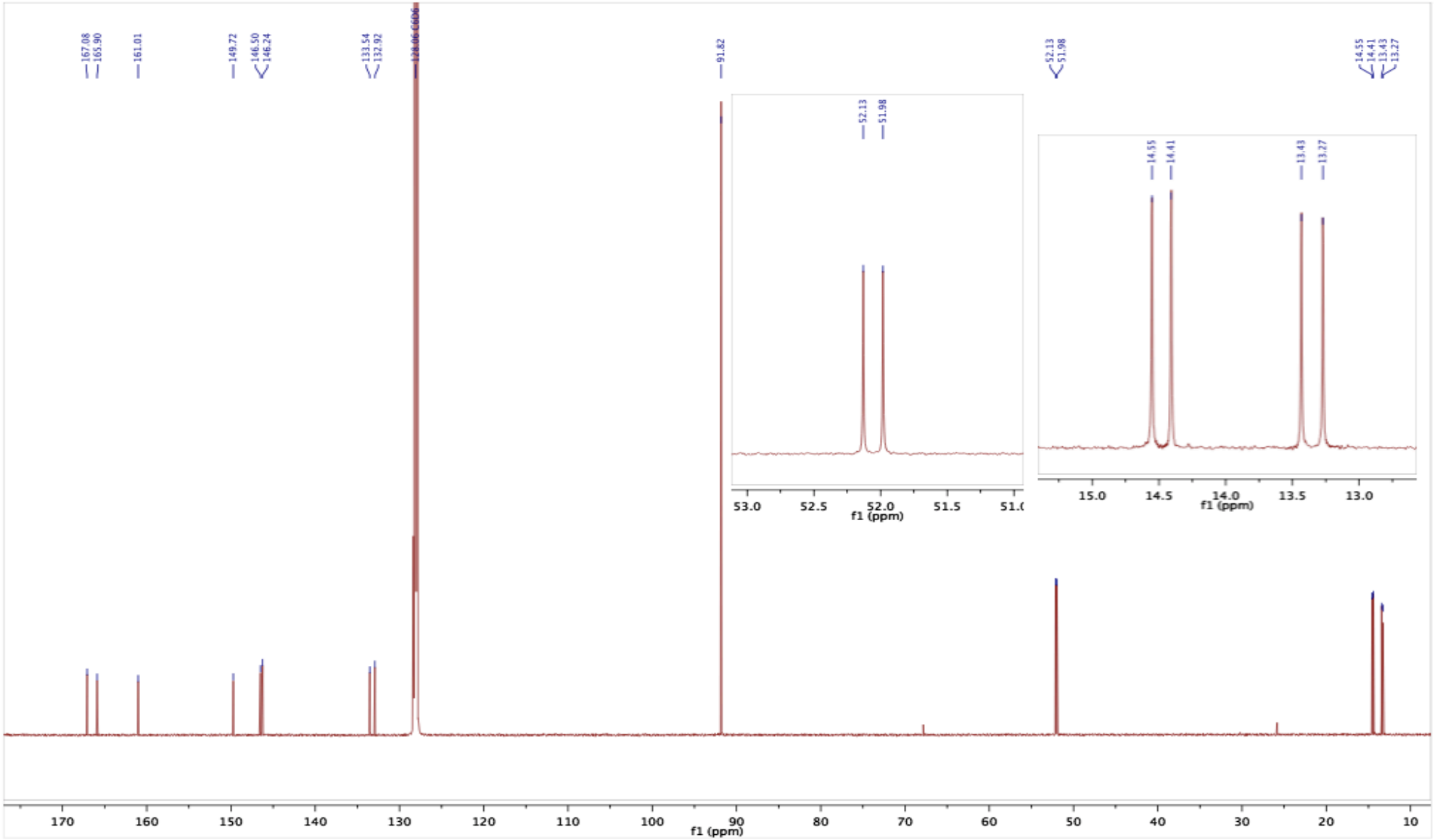

Figure S19. $^{13}C\{^{1}H\}$ NMR Spectrum (C_6D_6, 295 K, 202 MHz, δ) of [Mo{C(O)CR=CRAsC_4Me_4}$(CO)_2(\eta^5$-$C_5H_5)$] (R = CO_2Me, **7a**)

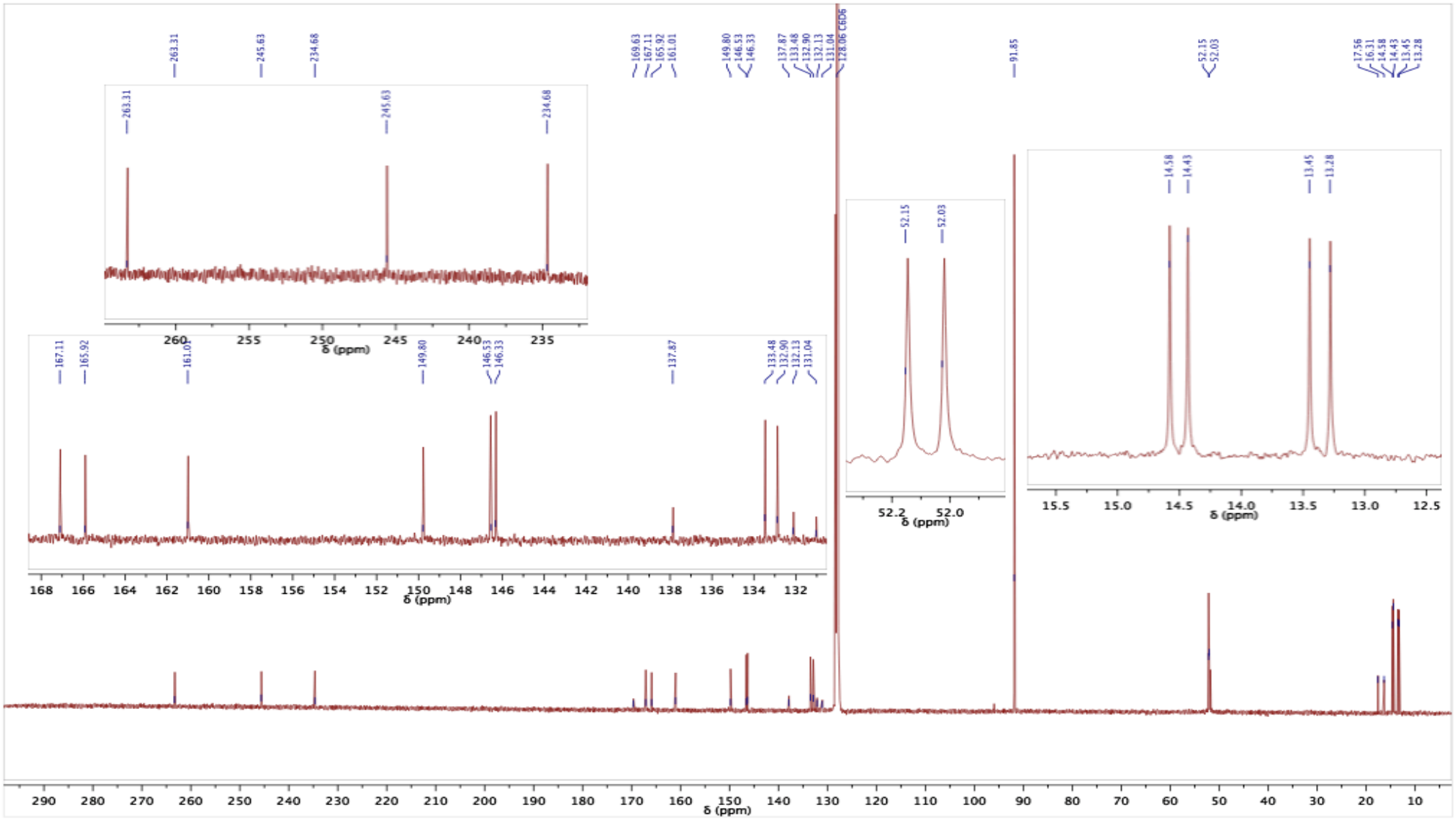

Figure S20. $^{13}C\{^{1}H\}$ NMR Spectrum (C_6D_6, 295 K, 101 MHz, δ) of [Mo{C(O)CR=CRAsC_4Me_4}$(CO)_2(\eta^5$-$C_5H_5)$] (R = CO_2Me, **7a**) (**x** = unreacted starting material)

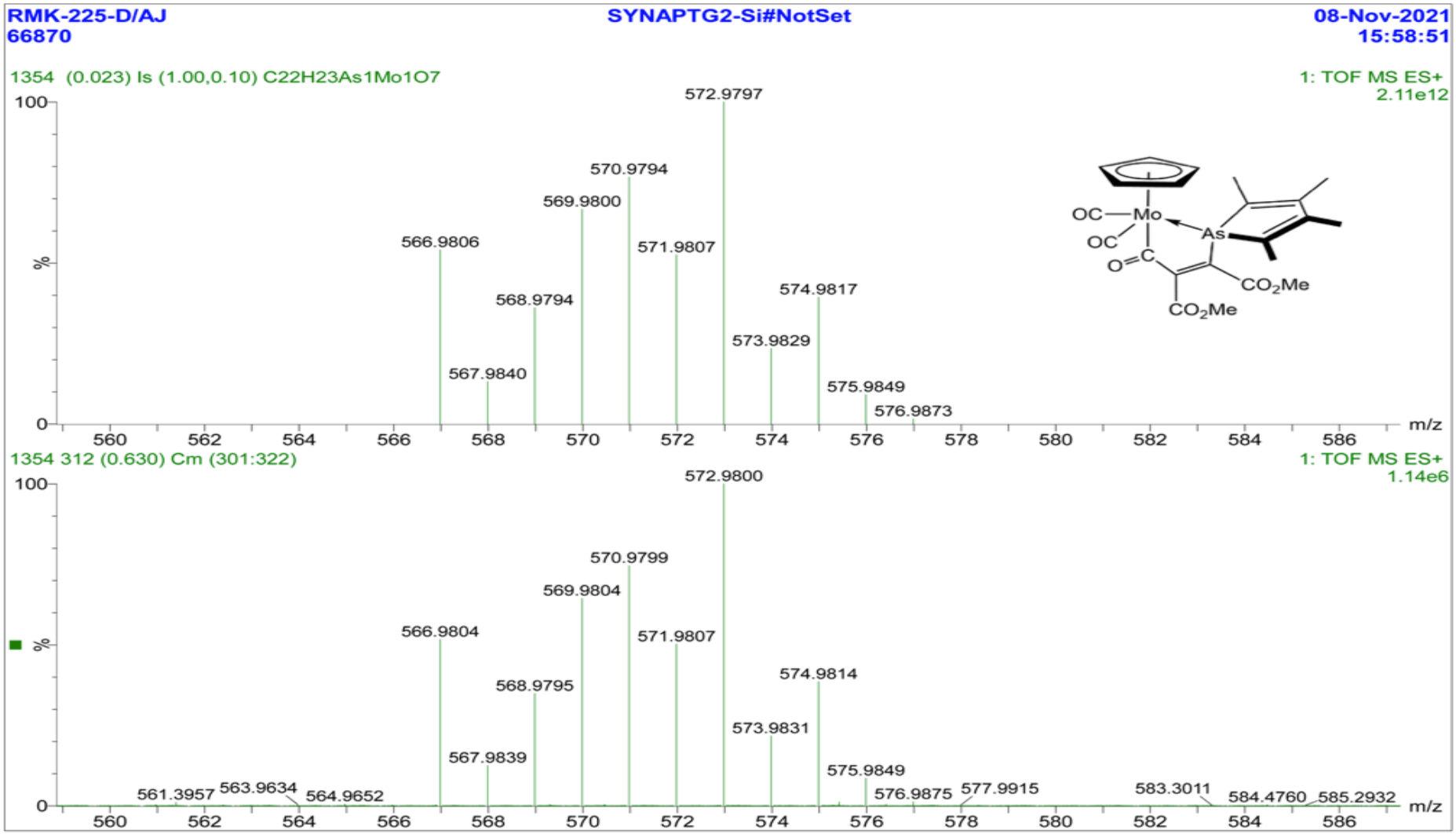

Figure S21. High Resolution Mass Spectrum (ESI-MS, MeCN, +ve ion) of $[Mo\{C(O)CR{=}CRAsC_4Me_4\}(CO)_2(\eta^5\text{-}C_5H_5)]$ (R = CO_2Me, **7a**)

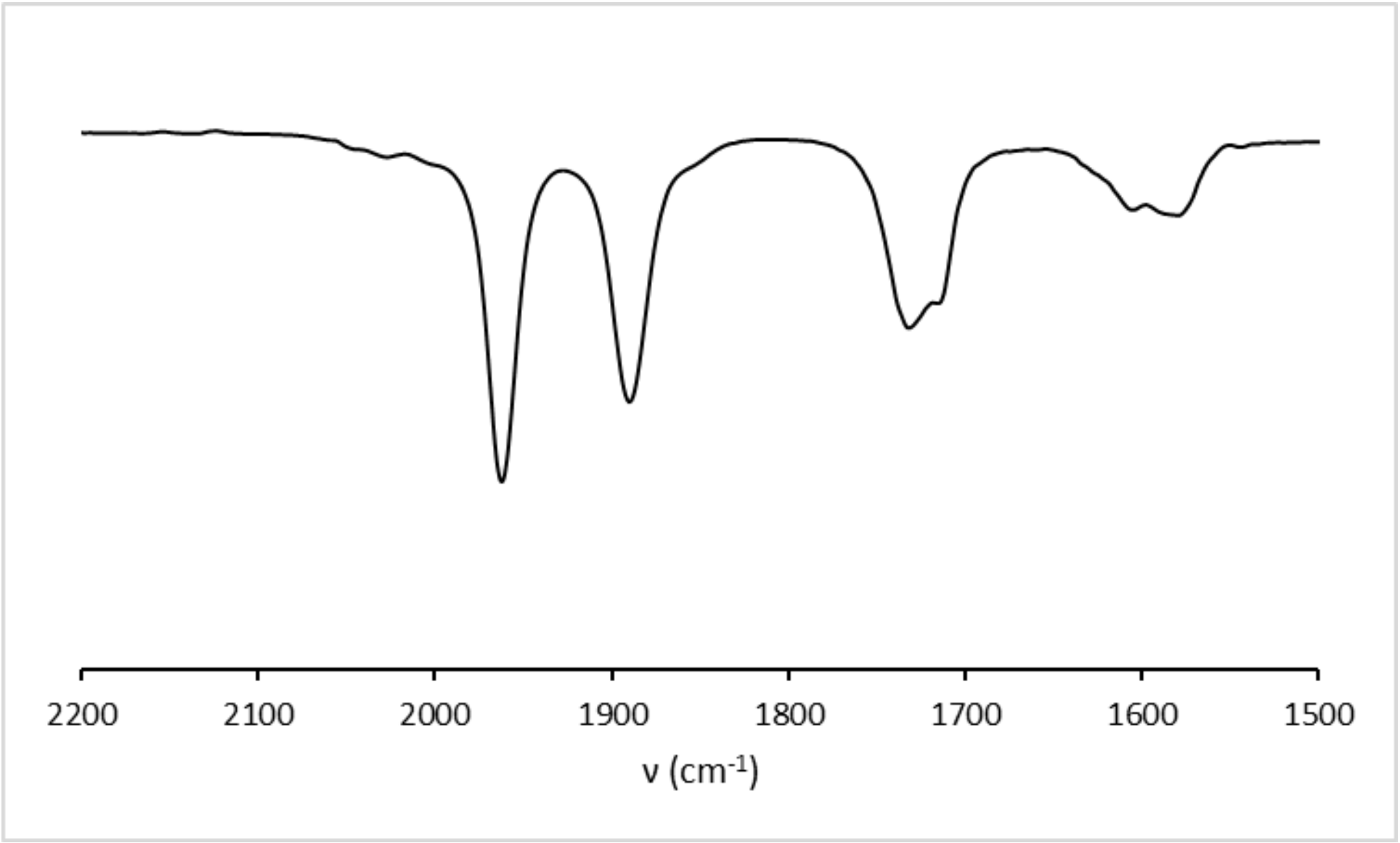

Figure S22. IR Spectrum (CH_2Cl_2, 295 K, ν cm^{-1}) of [Mo{C(O)CR=CRAsC_4Me_4}$(CO)_2(\eta^5$-$C_5H_5)$] (R = CO_2Me, **7a**)

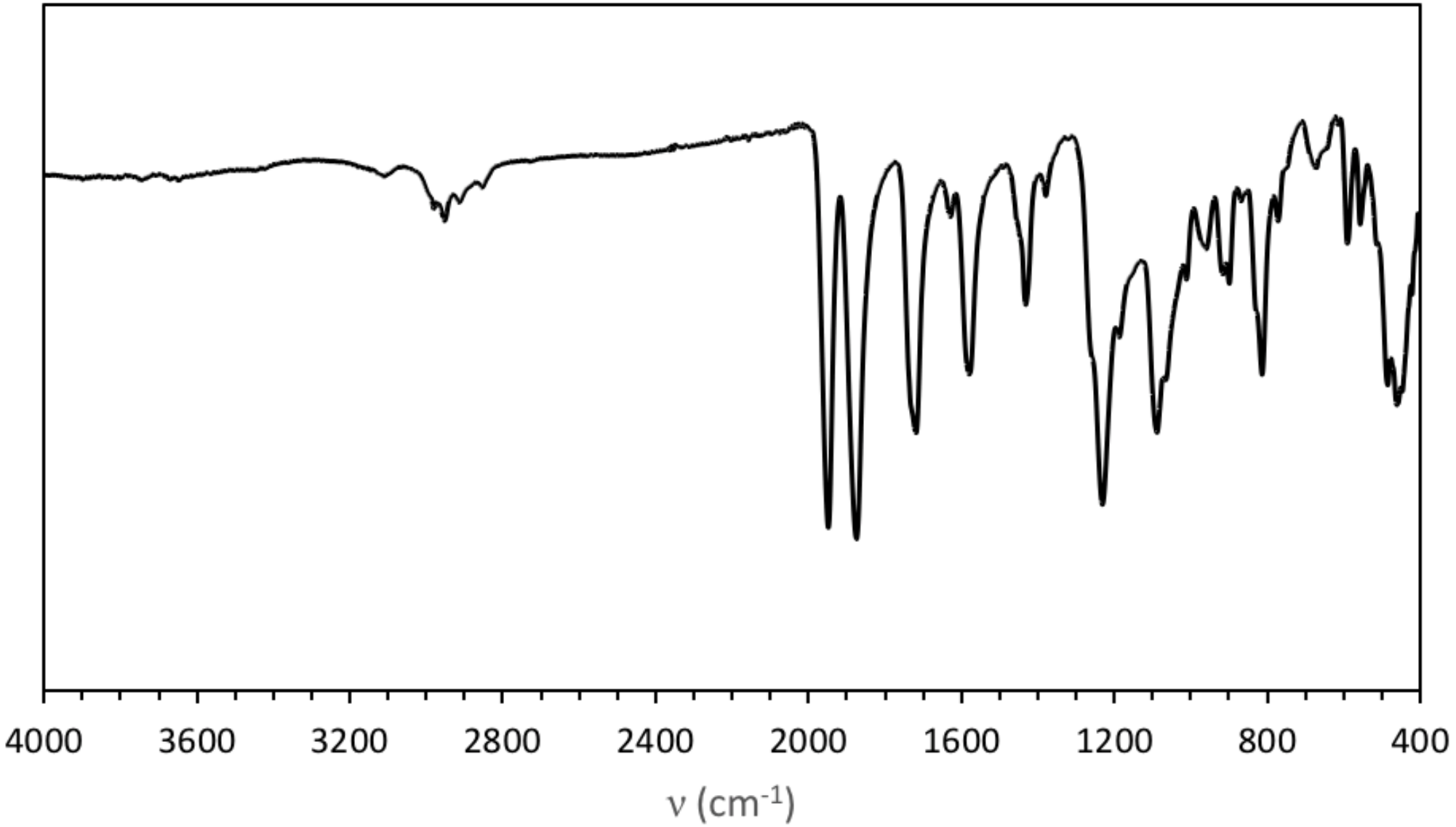

Figure S23. IR Spectrum (ATR, 295 K, ν cm^{-1}) of [Mo{C(O)CR=CRAsC_4Me_4}$(CO)_2(\eta^5$-$C_5H_5)$] (R = CO_2Me, **7a**)

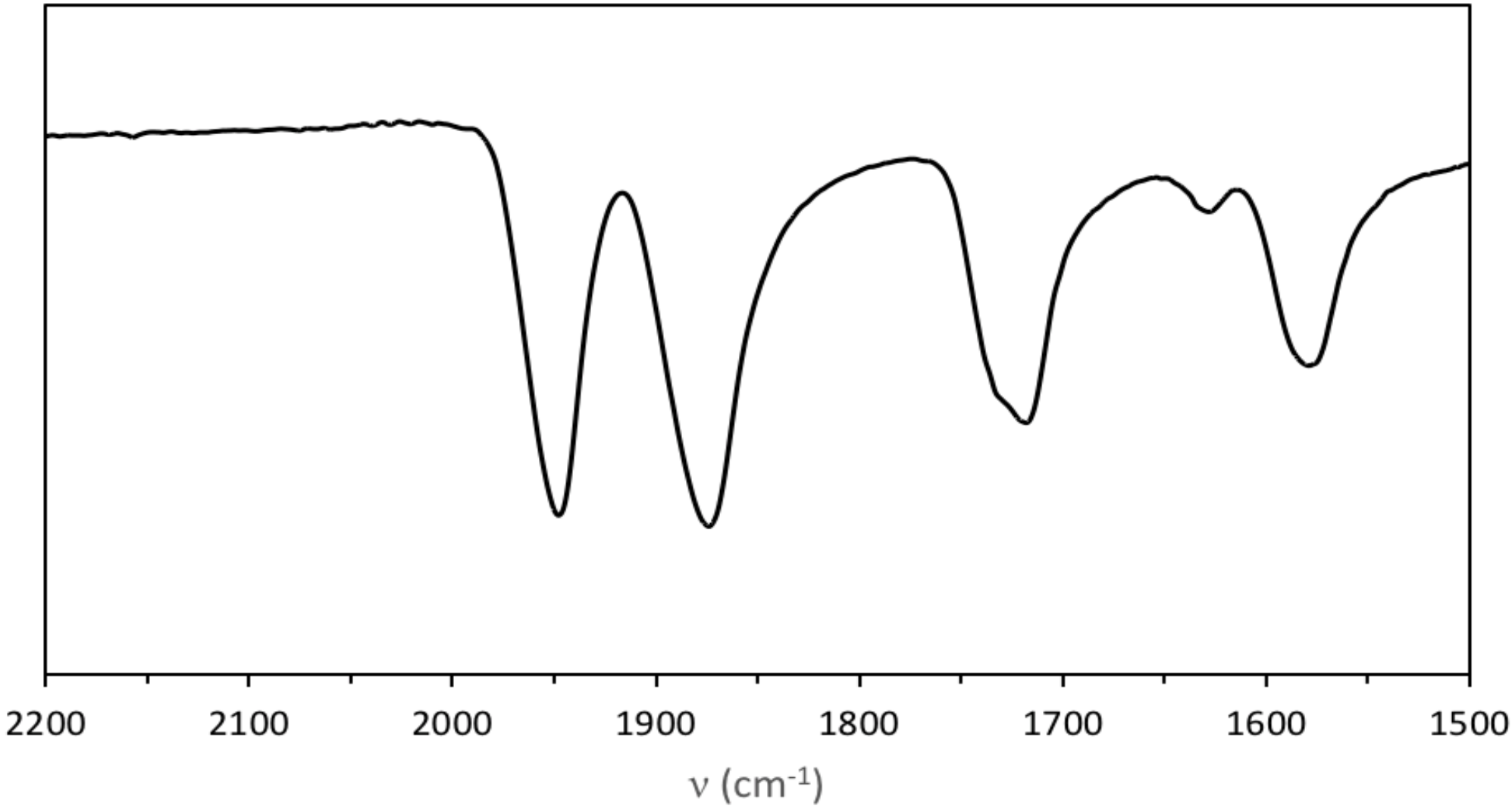

Figure S24. IR Spectrum (ATR, 295 K, ν cm^{-1}) of [Mo{C(O)CR=CRAsC_4Me_4}$(CO)_2(\eta^5$-$C_5H_5)$] (R = CO_2Me, **7a**) – ν_{CO} region expansion

4.6 [Mo{C(O)CR=CRAsC$_4$Me$_4$}(CO)$_2$(η^5-C$_5$H$_5$)] (R = CF$_3$, 7b)

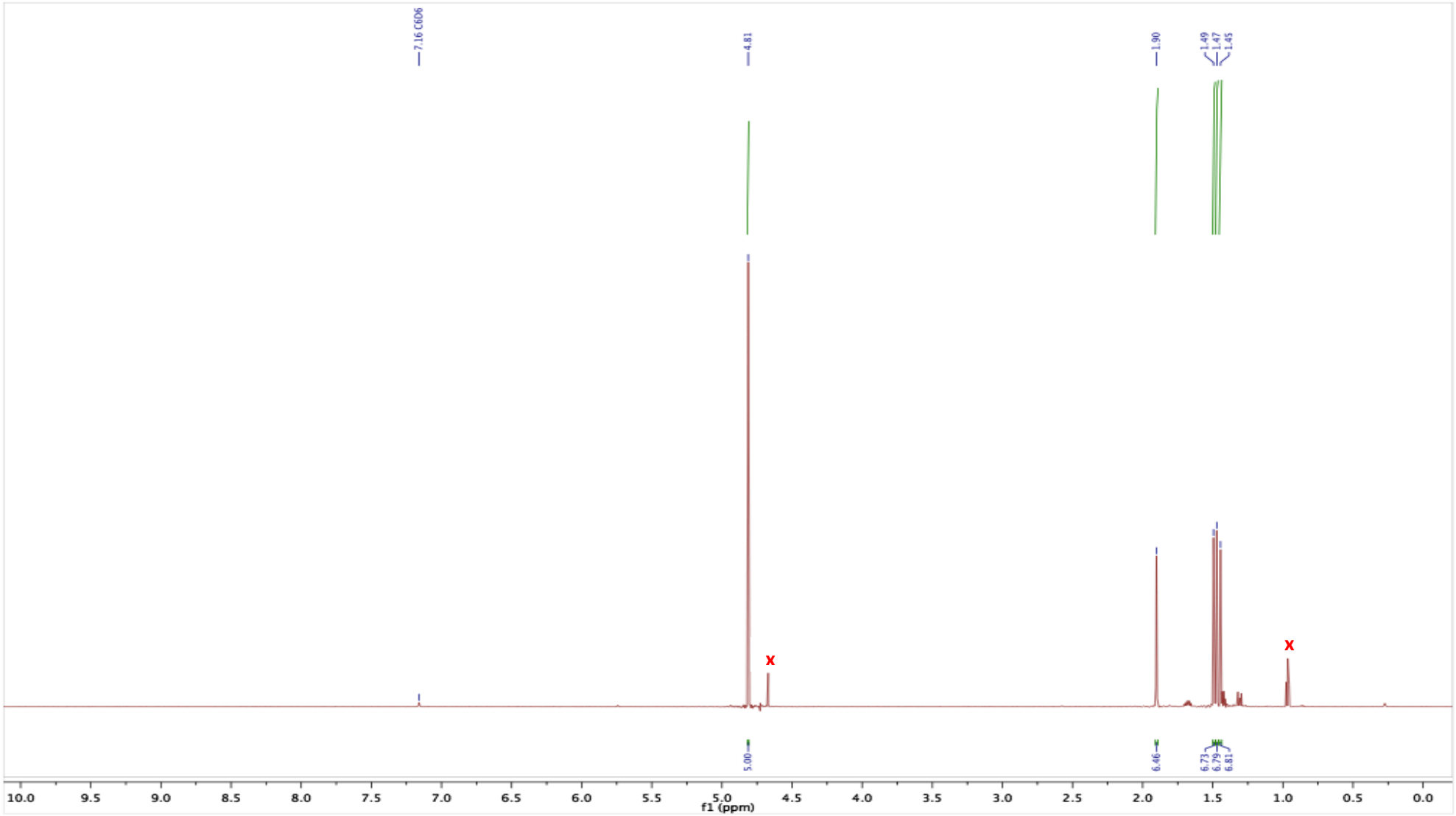

Figure S25. ^{1}H NMR Spectrum (CDCl$_3$, 295 K, 400 MHz, δ) of [Mo{C(O)CR=CRAsC$_4$Me$_4$}(CO)$_2$(η^5-C$_5$H$_5$)] (R = CF$_3$, **7b**, **x** = unidentified impurity)

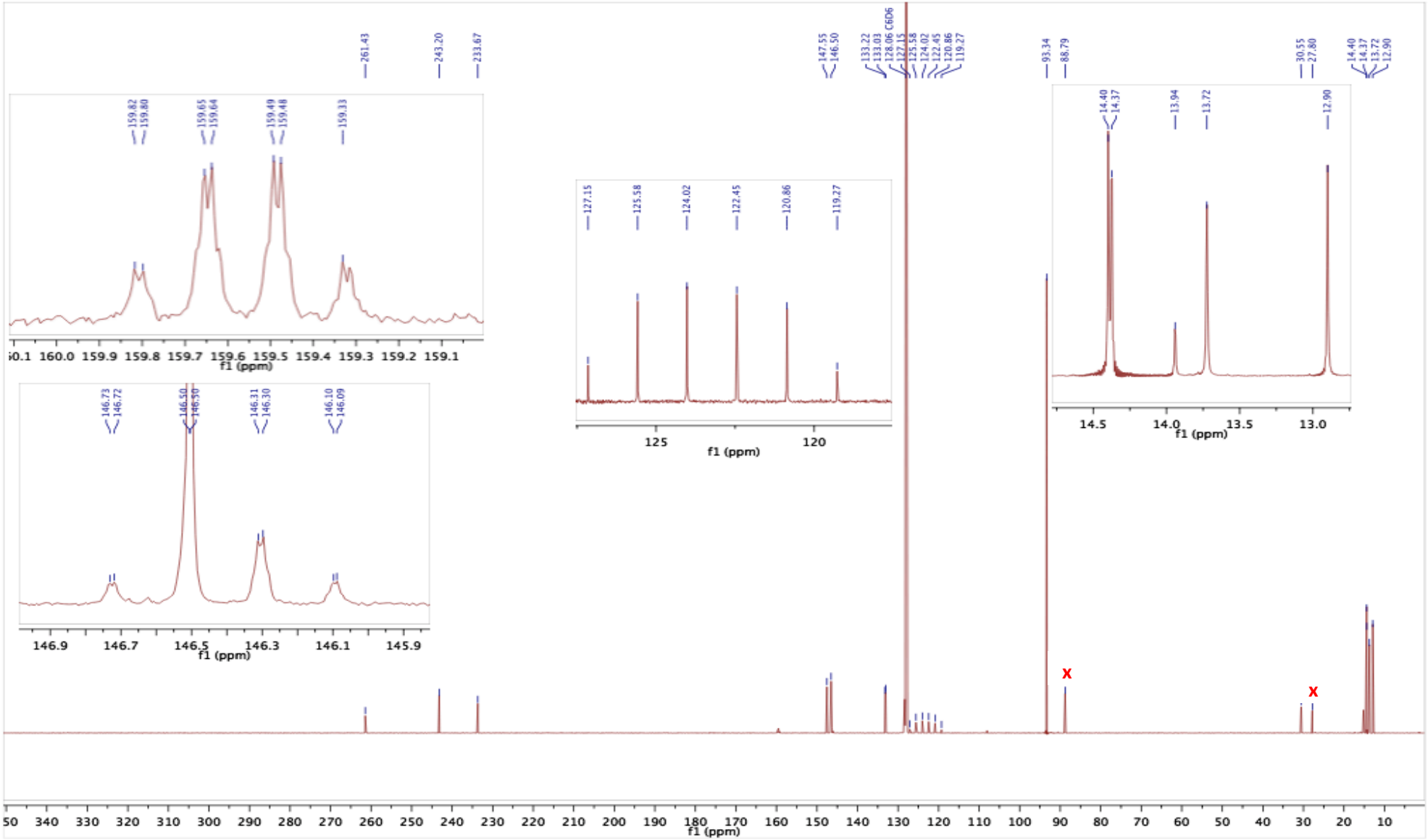

Figure S26. $^{13}C\{^{1}H\}$ NMR Spectrum (C_6D_6, 295 K, 202 MHz, δ) of [Mo{C(O)CR=CRAsC_4Me_4}$(CO)_2(\eta^5$-$C_5H_5)$] (R = CF_3, **7b**, x = unidentified impurity)

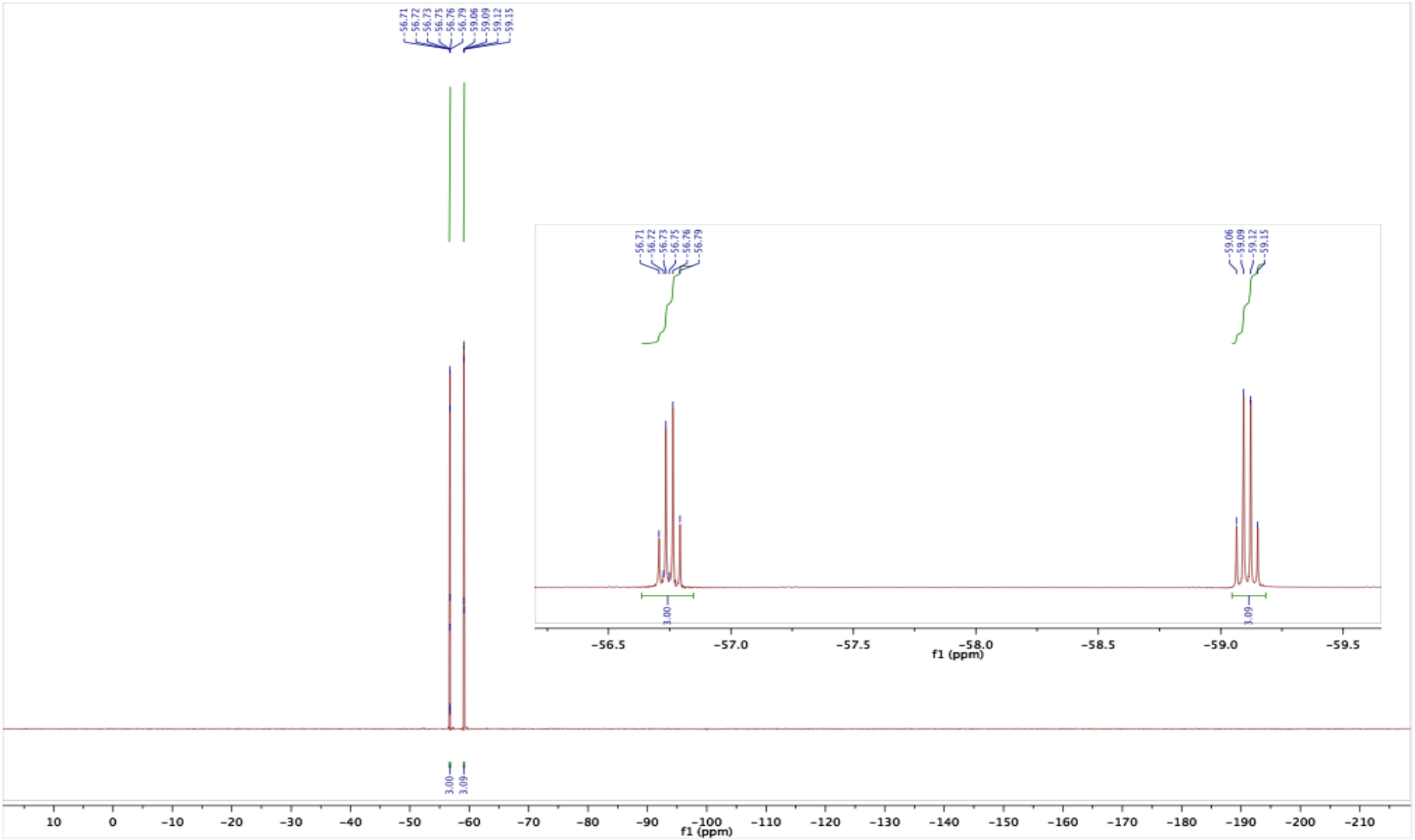

Figure S27. $^{19}F\{^{1}H\}$ NMR Spectrum (C_6D_6, 295 K, 376 MHz, δ) of [Mo{C(O)CR=CRAsC_4Me_4}$(CO)_2(\eta^5$-$C_5H_5)$] (R = CF_3, **7b**)

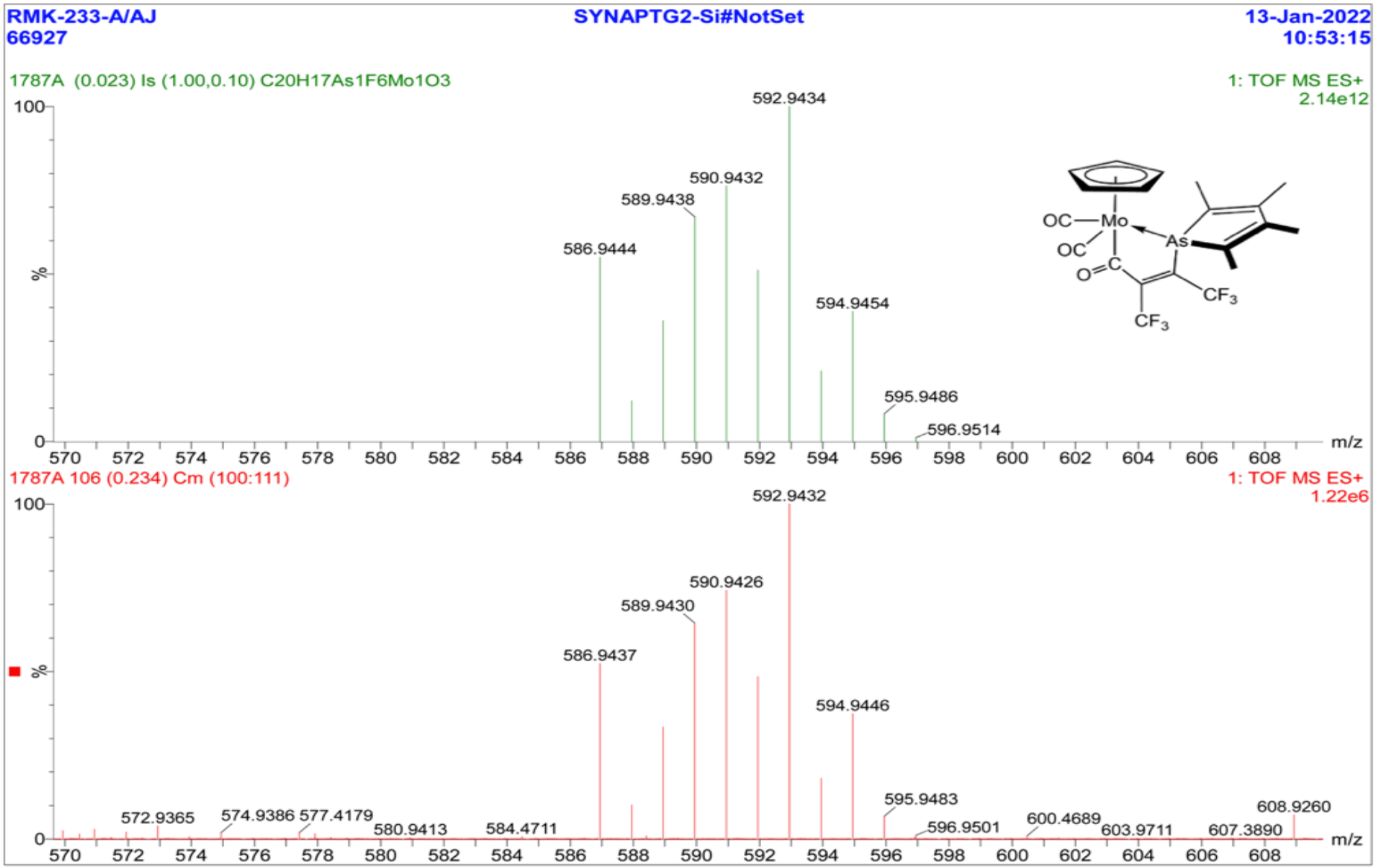

Figure S28. High Resolution Mass Spectrum (ESI-MS, MeCN) of [Mo{C(O)CR=CRAsC_4Me_4}$(CO)_2(\eta^5$-$C_5H_5)$] (R = CF_3, **7b**)

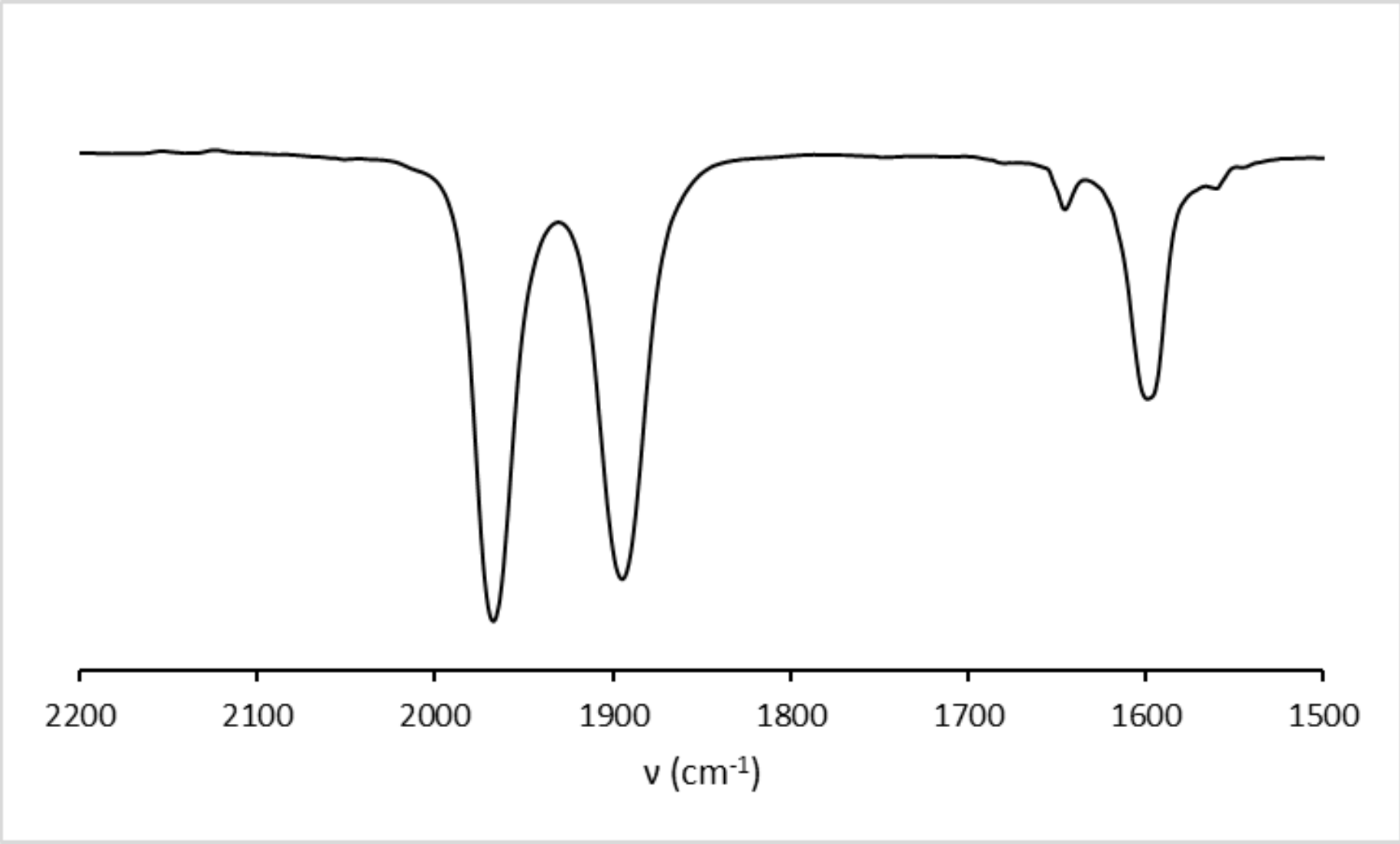

Figure S29. IR Spectrum (CH_2Cl_2, 295 K, ν cm^{-1}) of [Mo{C(O)CR=CRAsC_4Me_4}$(CO)_2(\eta^5$-$C_5H_5)$] ((R = CF_3, **7b**)

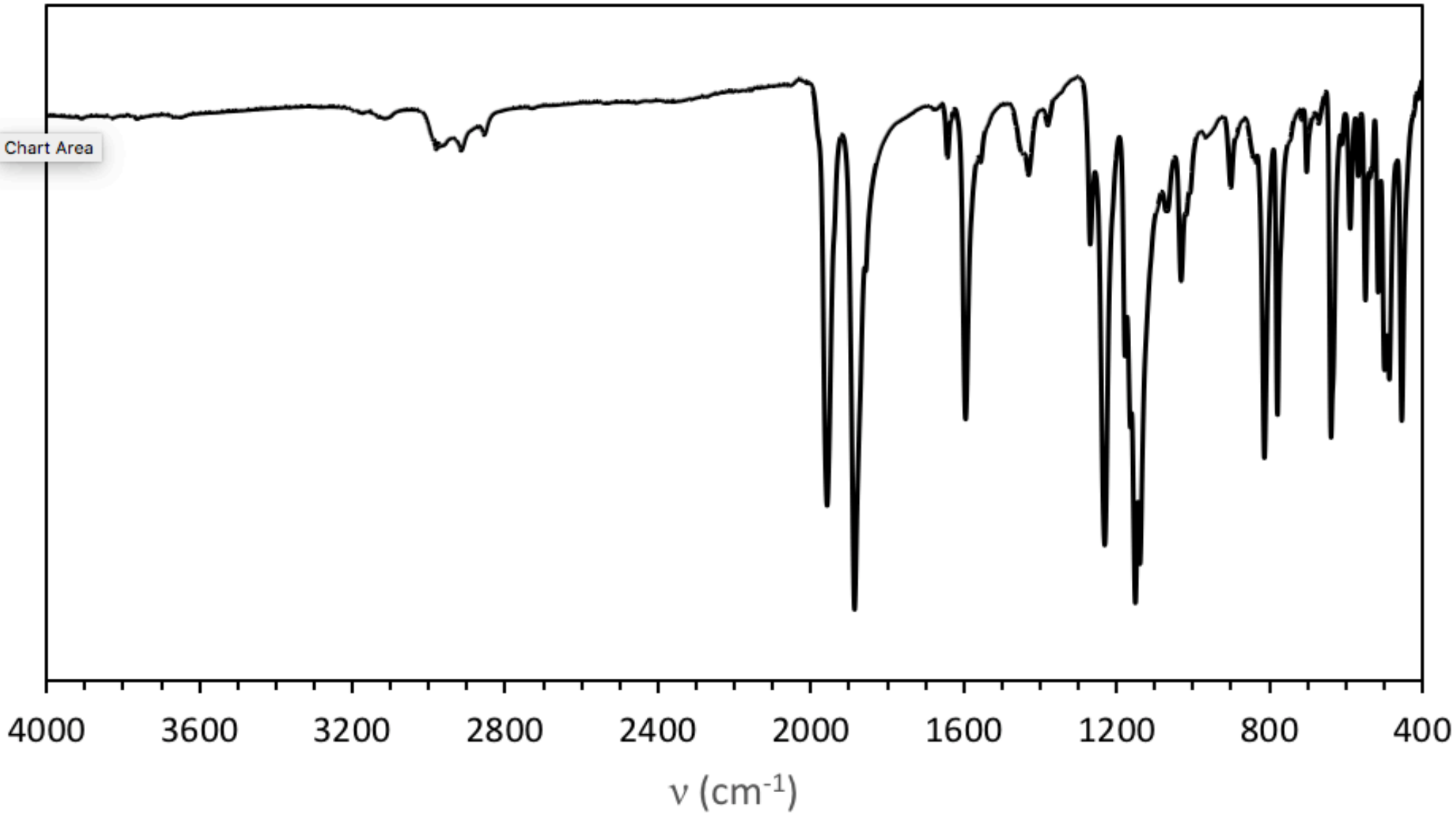

Figure S30. IR Spectrum (CH_2Cl_2, 295 K, ν cm^{-1}) of [Mo{C(O)CR=CRAsC_4Me_4}$(CO)_2(\eta^5$-$C_5H_5)$] ((R = CF_3, **7b**)

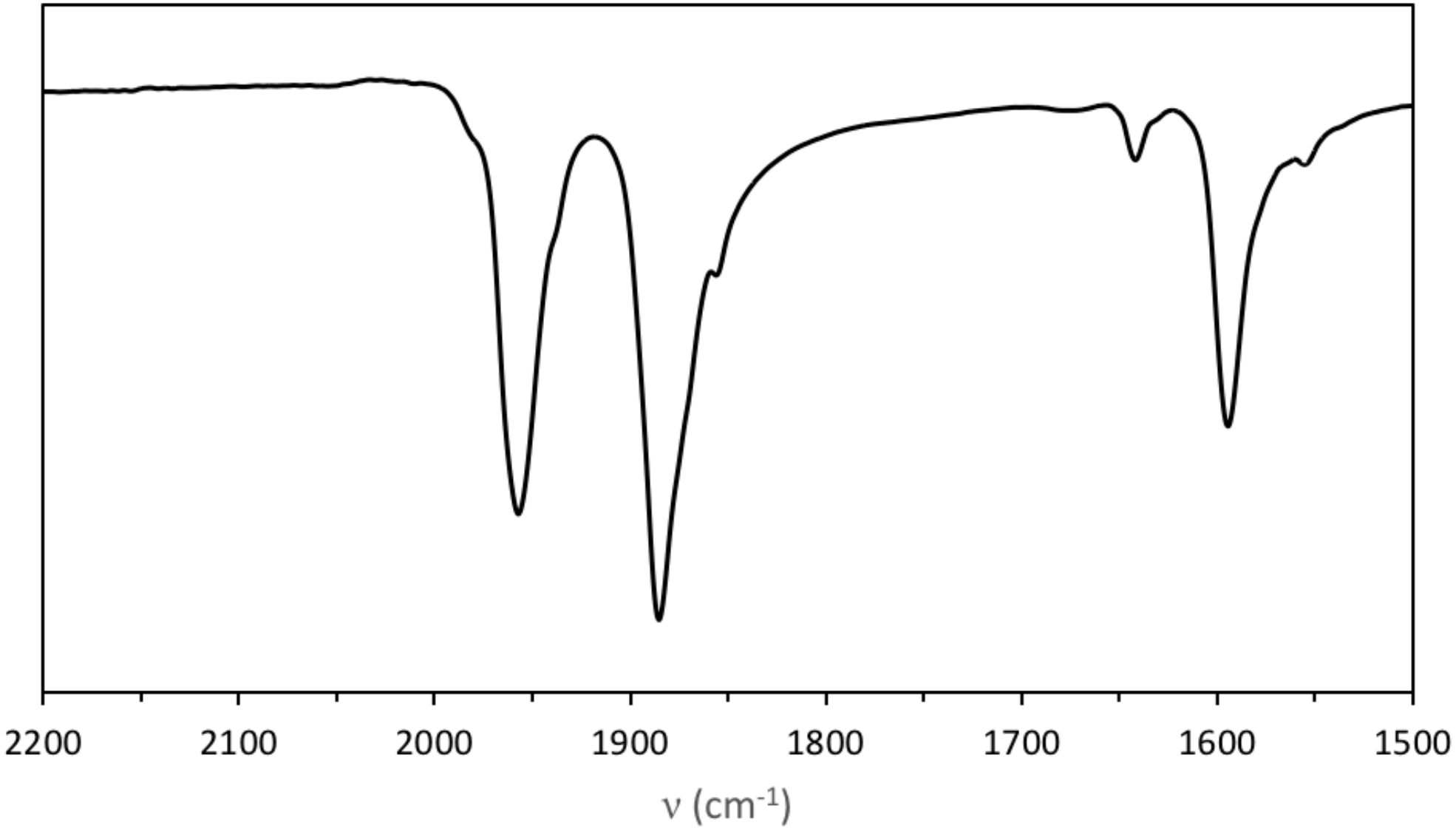

Figure S31 IR Spectrum (ATR, 295 K, ν cm^{-1}) of [Mo{C(O)CR=CRAsC_4Me_4}$(CO)_2(\eta^5$-$C_5H_5)$] ((R = CF_3, **7b**) – ν_{CO} region expansion

5 Computational Results

5.1 $Me_2AsC_4H_4$

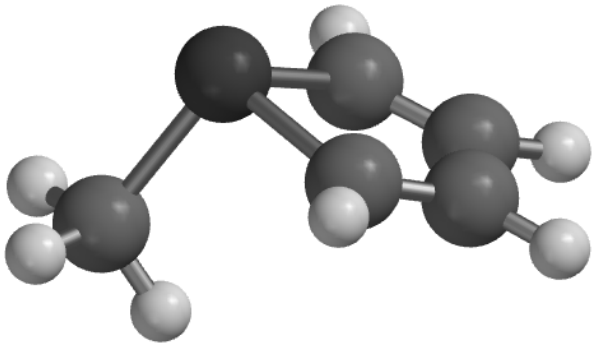

Figure S32. Optimised Geometry (wB97X-D/6-31G*/Gas Phase)

Thermodynamic Properties at 298.15 K

Zero Point Energy :	257.34	kJ/mol	(ZPE)
Temperature Correction :	19.18	kJ/mol	(vibration + gas law + rotation + translation)
Enthalpy Correction :	276.52	kJ/mol	(ZPE + temperature correction)
Enthalpy :	-2430.185364	au	(Electronic Energy + Enthalpy Correction)
Entropy :	334.93	J/mol•K	
Gibbs Energy :	-2430.223398	au	(Enthalpy - T*Entropy)
C_v :	106.75	J/mol•K	

Lowest energy vibrational mode = 124 cm^{-1}
Second lowest energy vibrational mode = 159 cm^{-1}.

Cartesian Coordinates

Atom	x	y	z
C	-1.236208	0.720351	0.371829
H	-1.733830	1.494889	0.945129
C	-1.348032	0.579099	-0.961268
H	-1.944414	1.241259	-1.585248
C	-0.609702	-0.541990	-1.551391
H	-0.636758	-0.722540	-2.623792
C	0.093044	-1.299994	-0.689578
H	0.684743	-2.162109	-0.977522
As	-0.209073	-0.732717	1.138827
C	1.498832	0.227947	1.434101
H	2.291448	-0.504741	1.604512
H	1.404602	0.853914	2.324708
H	1.745347	0.846630	0.569693

5.2 $[Me_2AsC_4H_4]+$

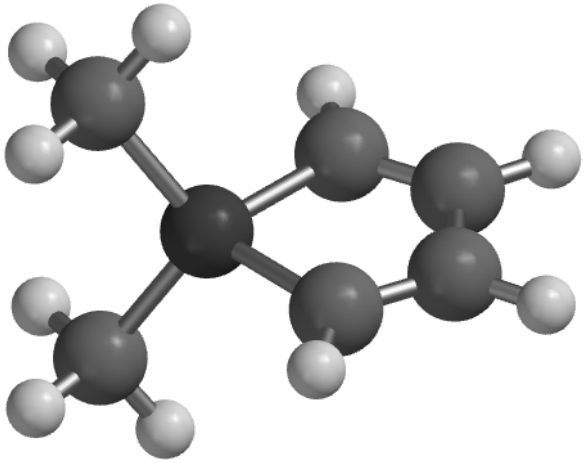

Figure S33. Optimised Geometry (wB97X-D/6-31G*/Gas Phase)

Thermodynamic Properties at 298.15 K

Zero Point Energy :	353.98	kJ/mol	(ZPE)
Temperature Correction :	23.64	kJ/mol	(vibration + gas law + rotation + translation)
Enthalpy Correction :	377.62	kJ/mol	(ZPE + temperature correction)
Enthalpy :	-2469.812298	au	(Electronic Energy + Enthalpy Correction)
Entropy :	367.78	J/mol•K	
Gibbs Energy :	-2469.854063	au	(Enthalpy - T*Entropy)
C_v :	140.40	J/mol•K	

Lowest energy vibrational mode = 105 cm^{-1}
Second lowest energy vibrational mode = 127 cm^{-1}.

Cartesian Coordinates

Atom	x	y	z
C	-1.015990	1.247631	-0.332357
H	-1.465603	2.059384	0.223887
C	-1.177209	0.982277	-1.635934
H	-1.805747	1.587058	-2.282431
C	-0.458958	-0.196615	-2.186038
H	-0.553615	-0.450180	-3.237423
C	0.292890	-0.910210	-1.337845
H	0.881874	-1.786841	-1.572782
As	0.158706	-0.078905	0.374019
C	1.829891	0.631163	1.009685
H	2.503673	-0.195599	1.244164
H	1.647746	1.224986	1.907850
H	2.263379	1.257789	0.228400
C	-0.661291	-1.189279	1.713681
H	0.013331	-2.012000	1.959658
H	-1.599826	-1.580726	1.317328
H	-0.853250	-0.589932	2.606137

5.3 [Mo{C(O)CH=CHAsC$_4$H$_4$)(CO)$_2$(η^5-C$_5$H$_5$)]

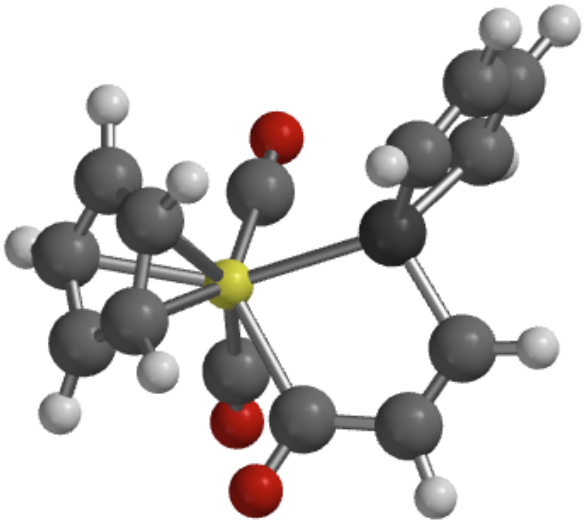

Figure S34. Optimised Geometry (wB97X-D/6-31G*/Gas Phase)

Cartesian Coordinates

Atom	x	y	z
Mo	0.998928	0.057017	-0.730222
C	-3.056978	1.185058	1.755623
C	-0.812993	1.658125	2.448018
O	1.473002	3.035655	0.163434
C	-2.528305	0.194884	1.022758
C	1.289754	1.935876	-0.145305
C	0.035802	0.821875	-2.746487
H	-0.345852	1.829114	-2.845023
C	0.145124	-1.441356	-2.376281
H	-0.124868	-2.457299	-2.126646
C	-0.721099	-0.318082	-2.375922
H	-1.775010	-0.326131	-2.131974
O	3.966375	-0.120262	0.243964
C	1.443761	-1.001813	-2.749351
H	2.316923	-1.631598	-2.842854
C	-2.106486	1.997156	2.541459
C	2.858600	-0.054473	-0.080603
C	1.378739	0.405559	-2.984472
H	2.189652	1.033744	-3.325827
H	-3.087125	-0.492016	0.398734
H	-4.122071	1.399072	1.792153
H	-2.464417	2.818525	3.156608
H	0.007024	2.158535	2.947774
As	-0.604419	0.194006	1.207839
C	1.232725	-1.903178	0.389954
C	0.635217	-2.180790	1.756217
H	0.937157	-3.119203	2.218552
C	-0.243722	-1.349707	2.305888
H	-0.741085	-1.509439	3.256824
O	1.825648	-2.818853	-0.144831

Thermodynamic Properties at 298.15 K

Zero Point Energy :	526.14	kJ/mol	(ZPE)
Temperature Correction :	45.16	kJ/mol	(vibration + gas law + rotation + translation)
Enthalpy Correction :	571.30	kJ/mol	(ZPE + temperature correction)
Enthalpy :	-3068.471408	au	(Electronic Energy + Enthalpy Correction)
Entropy :	523.67	J/mol•K	
Gibbs Energy :	-3068.530876	au	(Enthalpy - T*Entropy)
C_v :	309.02	J/mol•K	

Lowest energy vibrational mode = 25 cm^{-1}
Second lowest energy vibrational mode = 49 cm^{-1}.

Calculated[a] Allowed Electronic Transitions

nm ▼	strength	MO Component	%
301.58	0.0078	HOMO -> LUMO+2	49%
		HOMO -> LUMO+1	20%
319.42	0.0030	HOMO-2 -> LUMO+1	32%
		HOMO-2 -> LUMO	18%
		HOMO-2 -> LUMO+3	11%
		HOMO-1 -> LUMO+1	10%
335.05	0.0075	HOMO -> LUMO+1	69%
355.13	0.0008	HOMO-2 -> LUMO	27%
		HOMO -> LUMO	18%
		HOMO-2 -> LUMO+2	18%
		HOMO-1 -> LUMO	12%
367.05	0.0051	HOMO -> LUMO	53%
		HOMO -> LUMO+2	15%
415.76	0.0004	HOMO-1 -> LUMO+1	70%
		HOMO-2 -> LUMO+1	

[a]TD-DFT:ωB97X-D/6-31G*/LANL2Dζ/gas-phase

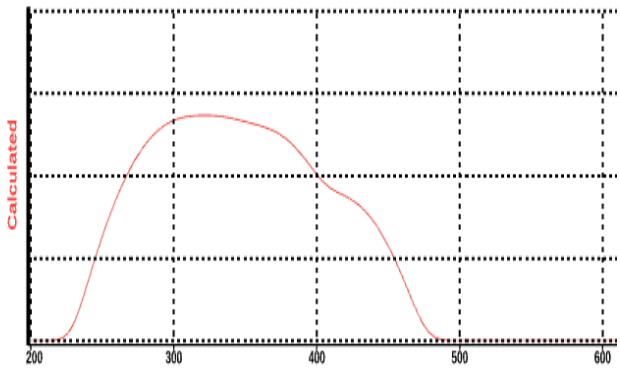

5.4 [Mo{C(O)C(CF$_3$)=C(CF$_3$)AsC$_4$H$_4$}(CO)$_2$(η^5-C$_5$H$_5$)]

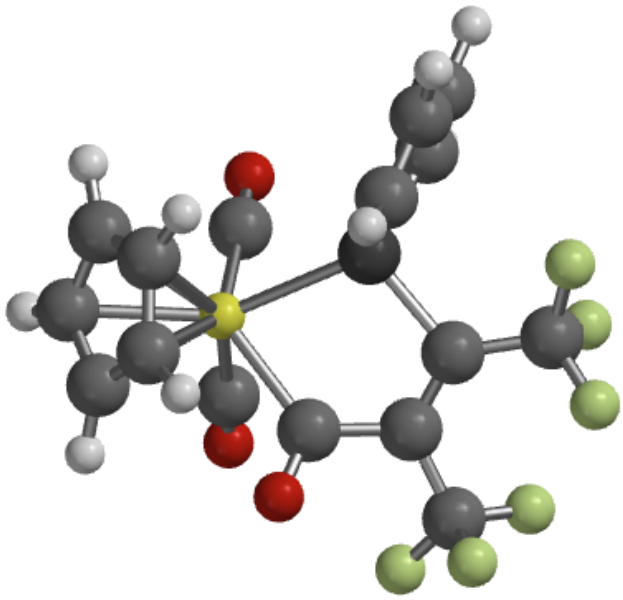

Figure S35. Transition State Geometry (wB97X-D/6-31G*/Gas Phase)

Thermodynamic Properties at 298.15 K

Zero Point Energy :	551.38	kJ/mol	(ZPE)
Temperature Correction :	59.85	kJ/mol	(vibration + gas law + rotation + translation)
Enthalpy Correction :	611.22	kJ/mol	(ZPE + temperature correction)
Enthalpy :	-3742.353270	au	(Electronic Energy + Enthalpy Correction)
Entropy :	624.68	J/mol•K	
Gibbs Energy :	-3742.424208	au	(Enthalpy - T*Entropy)
C_v :	415.27	J/mol•K	

Lowest energy vibrational mode = 19 cm^{-1}
Second lowest energy vibrational mode = 32 cm^{-1}.

Cartesian Coordinates

Atom	x	y	z
Mo	0.461035	-0.984048	-1.240560
C	1.532793	3.166035	0.891633
C	2.070201	1.002602	1.775097
O	3.225930	-1.769307	0.033909
C	0.485640	2.574384	0.300815
C	2.203382	-1.473964	-0.416959
C	1.567251	-0.236361	-3.200688
H	2.634351	-0.060154	-3.216753
C	-0.696468	0.100742	-3.004636
H	-1.657557	0.562769	-2.828581
C	0.571108	0.734178	-2.924577
H	0.752045	1.774440	-2.688656
O	-0.147399	-3.920139	-0.334818
C	-0.489685	-1.267047	-3.337076
H	-1.267695	-2.003369	-3.480307
C	2.408884	2.296992	1.702848
C	0.079321	-2.829334	-0.637808
C	0.919328	-1.477910	-3.461975
H	1.404843	-2.402046	-3.743244
H	-0.255300	3.063273	-0.319509
H	1.743483	4.228502	0.804686
H	3.275915	2.712504	2.208815
H	2.611449	0.233615	2.311194
As	0.553876	0.676617	0.634271
C	-1.536946	-0.982935	-0.255712
C	-1.744236	-0.675730	1.241634
C	-0.948909	0.233235	1.802110
O	-2.551348	-1.173705	-0.891618
C	-1.075965	0.845077	3.174861
C	-2.928764	-1.356857	1.903521
F	-0.484043	2.051404	3.213203
F	-2.347784	1.033194	3.540783
F	-0.477808	0.080197	4.097886
F	-2.725096	-1.525868	3.219445
F	-4.053830	-0.656017	1.741643
F	-3.112003	-2.574970	1.385122

Calculated[a] Allowed Electronic Transitions

nm	strength	MO Component	%
305.79	0.0048	HOMO -> LUMO+2	48%
		HOMO -> LUMO+3	20%
312.38	0.0075	HOMO-2 -> LUMO+1	45%
		HOMO-1 -> LUMO+1	20%
		HOMO-1 -> LUMO+2	12%
342.51	0.0043	HOMO -> LUMO+1	77%
351.73	0.0000	HOMO-2 -> LUMO	27%
		HOMO-1 -> LUMO	26%
		HOMO-1 -> LUMO+2	15%
		HOMO-2 -> LUMO+2	12%
366.66	0.0083	HOMO -> LUMO	63%
		HOMO -> LUMO+2	14%
407.01	0.0007	HOMO-1 -> LUMO+1	44%
		HOMO-2 -> LUMO+1	35%

[a]TD-DFT:ωB97X-D/6-31G*/LANL2DZ/gas-phase

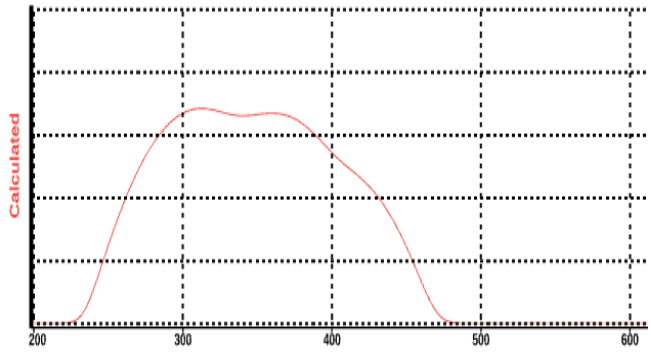

5.5 [Mo{C(O)C(CF$_3$)=C(CF$_3$)AsC$_4$Me$_4$)(CO)$_2$(η^5-C$_5$H$_5$)

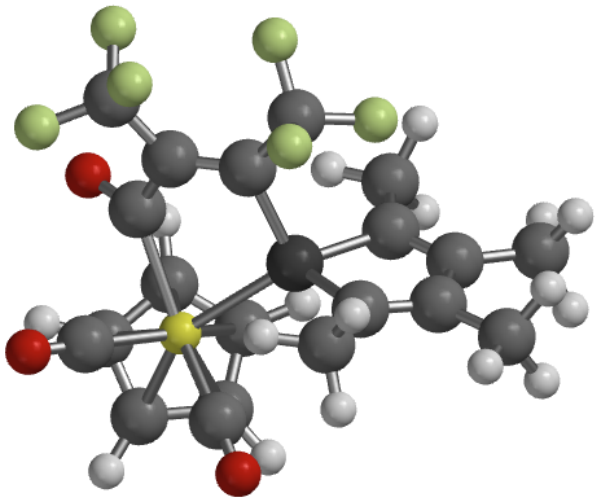

Figure S36. Optimised Geometry (ωB97X-D/6-31G*/Gas Phase)

Thermodynamic Properties at 298.15 K

Zero Point Energy :	830.68	kJ/mol	(ZPE)
Temperature Correction :	74.46	kJ/mol	(vibration + gas law + rotation + translation)
Enthalpy Correction :	905.15	kJ/mol	(ZPE + temperature correction)
Enthalpy :	-3899.481779	au	(Electronic Energy + Enthalpy Correction)
Entropy :	717.48	J/mol•K	
Gibbs Energy :	-3899.563256	au	(Enthalpy - T*Entropy)
C_v :	516.35	J/mol•K	

Lowest energy vibrational mode = 9 cm^{-1}
Second lowest energy vibrational mode = 30 cm^{-1}.

Calculated[a] Allowed Electronic Transitions

nm	Strength	MO_Component	%
307.56	0.0072	HOMO -> LUMO+2	21%
		HOMO-2 -> LUMO	19%
		HOMO -> LUMO+3	11%
		HOMO-1 -> LUMO	10%
311.75	0.0049	HOMO -> LUMO+2	22%
		HOMO -> LUMO+3	14%
		HOMO-2 -> LUMO	13%
		HOMO-2 -> LUMO+1	13%
338.17	0.0027	HOMO-1 -> LUMO+2	18%
		HOMO-2 -> LUMO+2	16%
		HOMO-1 -> LUMO+1	15%
		HOMO-2 -> LUMO+1	13%
341.90	0.0031	HOMO -> LUMO	55%
		HOMO -> LUMO+1	28%
350.14	0.0077	HOMO -> LUMO+1	29%
		HOMO -> LUMO+2	21%
		HOMO -> LUMO	16%
408.86	0.0008	HOMO-1 -> LUMO	48%
		HOMO-2 -> LUMO	32%

[a]TD-DFT:ωB97X-D/6-31G*/LANL2DZ/gas-phase

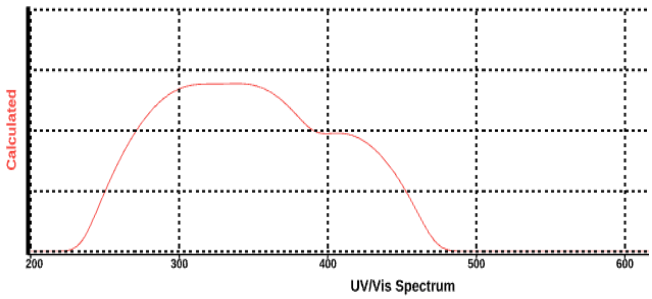

Frontier Orbitals of Relevance to UV-Vis Transitions

#	Label	Energy (eV)
134	LUMO{+2}	0.83
133	LUMO{+1}	0.11
132	LUMO	–0.13
131	HOMO	–7.65
130	HOMO{-1}	–7.89
129	HOMO{-2}	–8.04
128	HOMO{-3}	–8.35
127	HOMO{-4}	–9.43
126	HOMO{-5}	–9.85

Cartesian Coordinates

Atom	x	y	z
Mo	-1.606376	0.055508	-1.666905
C	2.417661	-1.146404	0.651439
C	0.178902	-1.502078	1.494010
O	-2.279564	-2.815744	-0.582478
C	1.918394	-0.092064	-0.021405
C	-2.021133	-1.748952	-0.945501
C	-0.732507	-0.959792	-3.616729
H	-0.434475	-1.999419	-3.626322
C	-0.652772	1.328762	-3.448406
H	-0.305353	2.337196	-3.274845
C	0.119215	0.143305	-3.352758
H	1.173457	0.087136	-3.119501
O	-4.558173	0.508236	-0.732738
C	-1.987233	0.967028	-3.774698
H	-2.807109	1.654492	-3.927869
C	1.457364	-1.923483	1.491671
C	-3.458847	0.339794	-1.046271
C	-2.039982	-0.456467	-3.884577
H	-2.903246	-1.045527	-4.161226
As	0.016639	-0.049953	0.247548
C	-1.680201	2.041237	-0.652632
C	-1.348761	2.258794	0.836738
C	-0.408816	1.486653	1.379058
O	-1.933826	3.047988	-1.279596
C	2.658890	0.896384	-0.873321
H	1.975078	1.607589	-1.346731
H	3.231584	0.406196	-1.670262
H	3.365842	1.478780	-0.271224
C	3.868233	-1.537884	0.633437
H	3.994438	-2.579303	0.316055
H	4.306847	-1.451524	1.634694
H	4.449534	-0.905637	-0.041344
C	1.950939	-3.085267	2.306869
H	1.138637	-3.554922	2.865570
H	2.715170	-2.765853	3.025148
H	2.407189	-3.851293	1.669184
C	-0.976220	-2.040467	2.286505
H	-1.883546	-1.453318	2.118714
H	-0.759710	-2.007769	3.359710
H	-1.206353	-3.076010	2.012895
C	0.223243	1.630579	2.740744
C	-2.050210	3.424166	1.511359
F	1.454116	1.088099	2.754951
F	0.369289	2.905593	3.116230
F	-0.498225	0.994800	3.676345
F	-2.190770	3.215574	2.830640
F	-1.384070	4.569376	1.339614
F	-3.283183	3.575863	1.018211

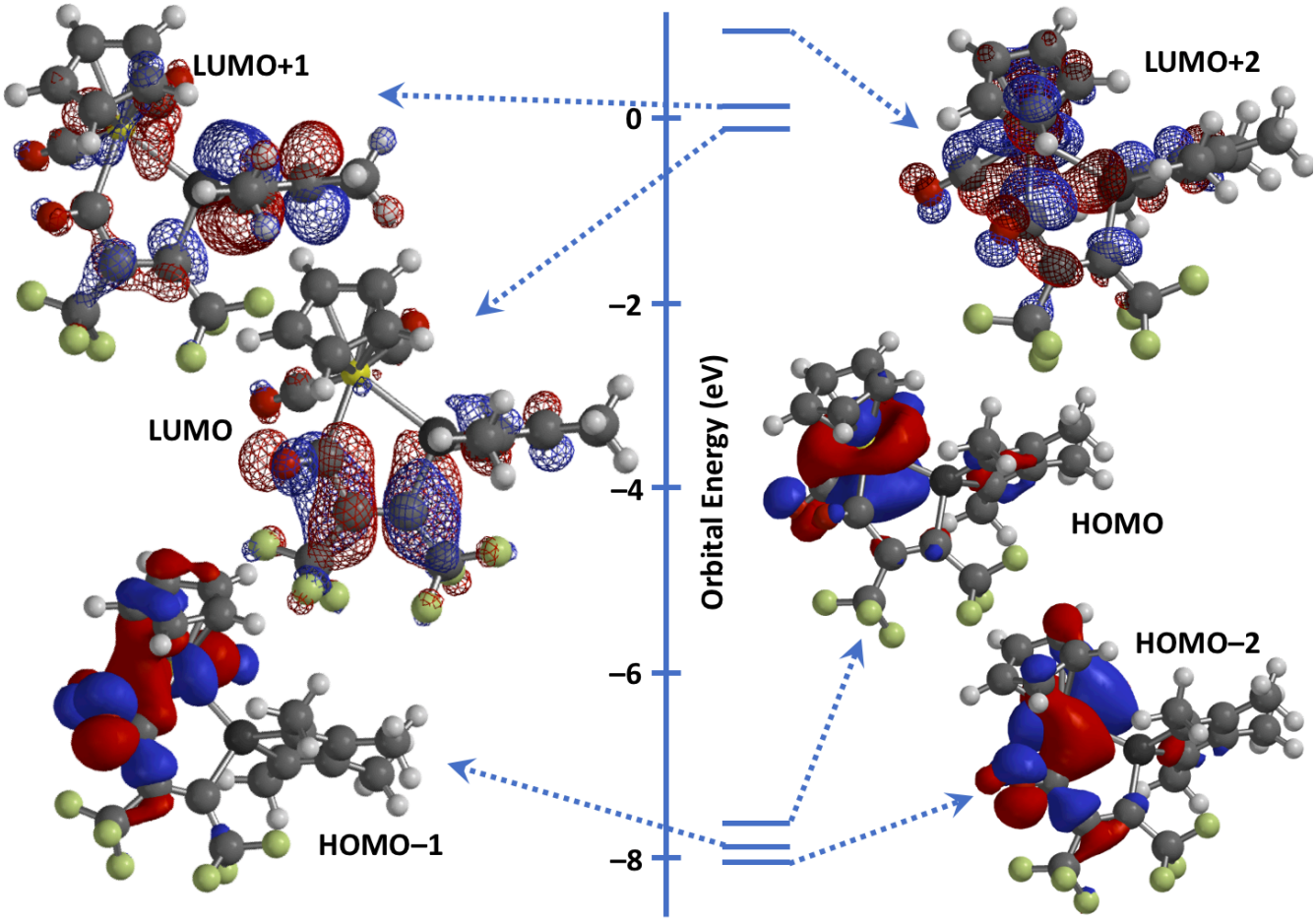

Figure S37. Frontier Molecular Orbitals Relevant to Allowed Electronic Transitions (TD-DFT:ωB97X-D/6-31G*/LANL2Dζ/gas-phase).